

To appear in J. G. R., Oct. 1974

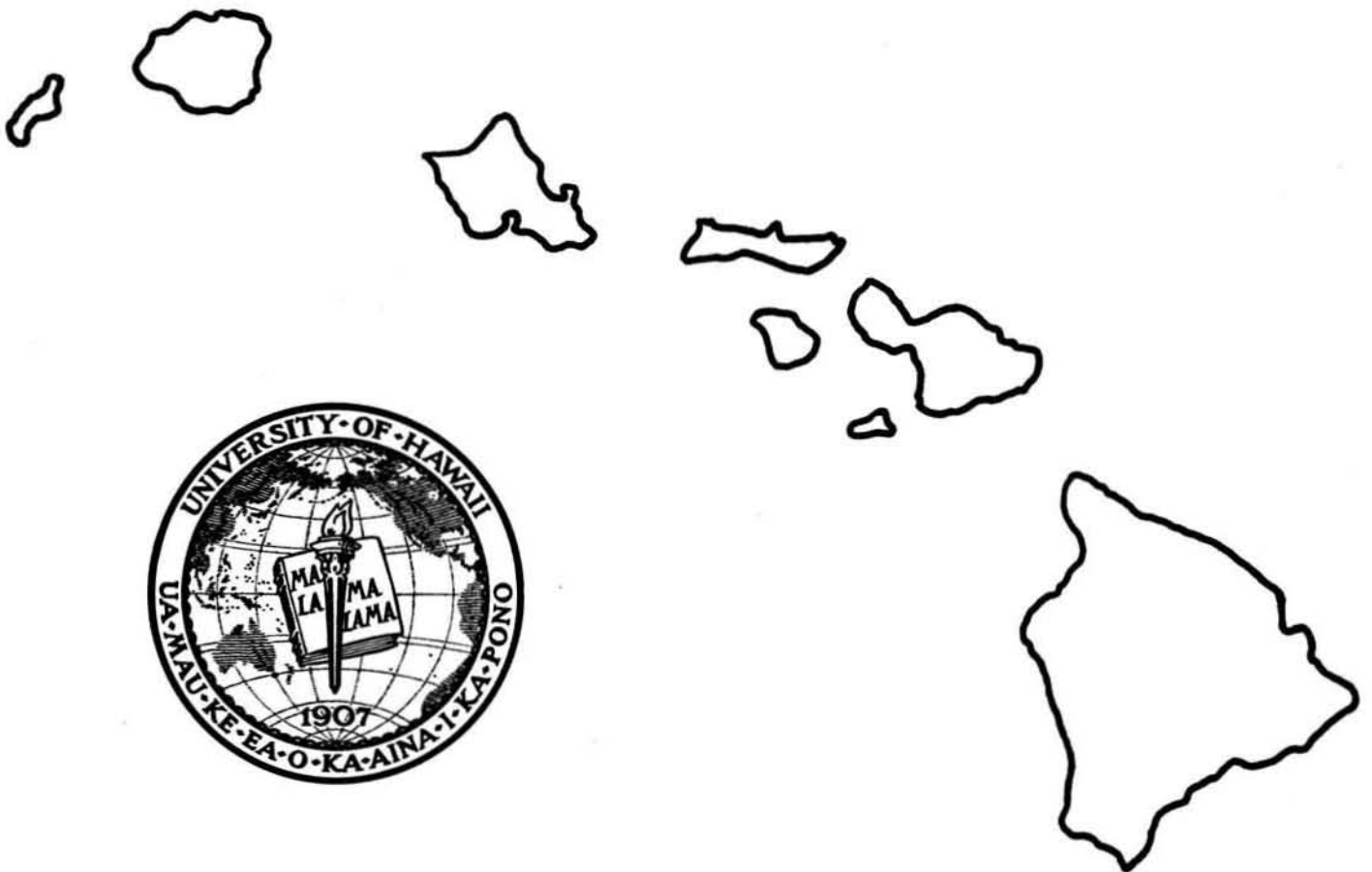
K

THE HAWAII GEOTHERMAL PROJECT

STEADY STATE FREE CONVECTION
IN AN UNCONFINED GEOTHERMAL RESERVOIR

TECHNICAL REPORT No. 2

March 1, 1974



HAWAII GEOTHERMAL PROJECT
ENGINEERING PROGRAM

STEADY STATE FREE CONVECTION
IN AN UNCONFINED GEOTHERMAL RESERVOIR
TECHNICAL REPORT No. 2

March 1, 1974

Prepared Under
NATIONAL SCIENCE FOUNDATION
RESEARCH GRANT NO. GI-38319

By
Ping Cheng
K. H. Lau

Hilo College
University of Hawaii
Hilo, Hawaii 96720

College of Engineering
University of Hawaii
Honolulu, Hawaii 96822

TABLE OF CONTENTS

	<u>Page No.</u>
Abstract	i
List of Symbols	ii
List of Figures	iv
Introduction	1
Governing Equations and Boundary Conditions	2
Perturbation Analysis	6
Zero-Order Approximations	6
First-Order Approximations	8
Numerical Computations and Results	10
Concluding Remarks	14
Acknowledgment	16
References	17
Figures	18
Appendix A. Alternative Formulation in Terms of Stream Function	34
Appendix B. Finite Difference Equations	37
Appendix C. Computer Programs	45

STEADY STATE FREE CONVECTION IN AN UNCONFINED GEOTHERMAL RESERVOIR

Ping Cheng
Department of Mechanical Engineering
University of Hawaii
Honolulu, Hawaii

K. H. Lau
Hilo College
University of Hawaii
Hilo, Hawaii

Abstract. The problem of steady state free convection in an unconfined coastal aquifer with non-isothermal geothermal heating from below is investigated in this paper. The governing non-linear partial differential equations with non-linear boundary conditions are approximated by a set of linear sub-problems on the basis of the perturbation method. The equations for the zero-order and first-order approximations are of the elliptic type that can be solved numerically by the finite difference method. Numerical results, accurate to the first-order approximations, are obtained for temperature, pressure and stream function as well as for the shape of the water table. The influence of the location and the size of the heat source as well as various parameters on heat transfer and fluid flow characteristics in a rectangular geothermal aquifer is discussed.

List of Symbols

$D,$	discharge number, $D \equiv \rho_s Kgh/\alpha\mu$
$g,$	gravity vector
$h,$	height of the reservoir at the ocean sides
$k_m,$	thermal conductivity of the porous medium
$K,$	permeability of the porous medium
$\ell,$	the width of the reservoir
$L,$	the dimensionless width of the reservoir, $L \equiv \ell/h$
$m,$	dummy index in Eqs. (23)
$p,$	pressure
$P,$	dimensionless pressure, $P \equiv (p-p_a) / \rho_s gh$
P_0, P_1	zero-order and first-order perturbation functions for pressure
$T,$	temperature
$T_c,$	maximum temperature of the impermeable surface
T_L	prescribed temperature of the impermeable surface
$u, v,$	velocity components in the x and y directions
$x, y,$	Cartesian coordinate system
$X, Y,$	dimensionless coordinates
$\alpha,$	equivalent thermal diffusivity, $\alpha \equiv k_m/(\rho C_p)_f$
$\beta,$	thermal expansion coefficient
$\epsilon,$	perturbation parameter, $\epsilon \equiv \beta (T_c - T_s)$
$\eta,$	the height of water table
$\bar{\eta},$	dimensionless height of water table, $\bar{\eta} \equiv \eta/h$
η_1, η_2	zero-order and first-order perturbation functions for the height of water table
$\theta,$	dimensionless temperature, $\theta \equiv (T - T_s) / (T_c - T_s)$
θ_0, θ_1	zero-order and first-order perturbation functions for temperature

θ_L , prescribed dimensionless temperature of the impermeable surface

μ , viscosity of convecting fluid

ρ , density of convecting fluid

Subscripts

a, atmospheric condition

s, condition in the ocean

List of Figures

- Fig. 1a Coastal Unconfined Aquifer with Thermal Source
- Fig. 1b Rectangular Model of Aquifer
- Fig. 2 Contours of First-Order Perturbation for Stream Function
- Fig. 3a Contours of First-Order Perturbation Function for Pressure
- Fig. 3b Pressure Contours for Case 1
- Fig. 4a Contours of Zero-Order Perturbation Function for Temperature
- Fig. 4b Effect of Discharge Number on the Contours of First-Order Perturbation Function of Temperature
- Fig. 4c Effect of Discharge Number on Temperature Contours for Case 1
- Fig. 5a Effect of Discharge Number on the Horizontal Temperature Distribution for Case 1
- Fig. 5b Effect of the Location of Heat Source on the Horizontal Temperature Distribution
- Fig. 5c Effect of the Size of the Heat Source on the Horizontal Temperature Distribution
- Fig. 6a Effect of Discharge Number on Vertical Temperature Profiles for Case 1
- Fig. 6b Effect of Discharge Number on Vertical Temperature Profiles for Case 2
- Fig. 6c Effect of the Location of the Heat Source on Vertical Temperature Profiles
- Fig. 6d Effect of the Size of the Heat Source on Vertical Temperature Profiles
- Fig. 7a Effect of the Location of the Heat Source on the First-Order Perturbation Function for the Upwelling of Water Table
- Fig. 7b Effect of the Size of the Heat Source on the First-Order Perturbation Function for the Upwelling of Water Table

Introduction. Over the past two decades much work has been done on convective heat transfer in a porous medium. *Horton and Rogers* [1945] studied the criterion for the onset of free convection in a porous medium. This was followed by a series of papers by *Lapwood* [1948], *Wooding* [1961], and *Katto and Masuoka* [1967] on the same topics.

In recent years the utilization of geothermal energy for power production has stimulated further interest in the study of heat transfer and fluid flow characteristics in geothermal reservoirs. *Wooding* [1957] obtained a numerical solution for the prediction of temperature distribution in a two-dimensional geothermal reservoir at Wairakai, New Zealand. *Donaldson* [1962] considered steady state free convection in a two-dimensional porous medium bounded by isothermal horizontal impermeable walls. The effects of a non-isothermal wall on free convection was considered by *Elder* [1967a, 1967b]. The related problem of combined free and forced convection in a porous medium was treated by *Pratt* [1966] as well as by *Combarous and Bia* [1971]. The three-dimensional problem of free convection in a porous medium inside a rectangular enclosure was studied by *Chan et al* [1970], *Holst and Aziz* [1972a, 1972b] and by *Bories and Combarous* [1973]. The more complicated problem of circulation patterns of groundwater effected by geothermal heating was considered by *Henry and Kohout* [1973] in their study on waste disposal. All of the preceding studies concern a porous medium bounded by impermeable walls which are applicable to confined geothermal reservoirs.

In the island of Hawaii, as in many parts of the world, geothermal reservoirs are believed to be unconfined at the top. It has been speculated that upwelling of the water table as observed by *Keller* [1974] is possibly due to geothermal heating. Furthermore, the porosity of the island rock permits free flow of the water between the ocean and the island. This will undoubtedly affect the temperature distribution in the geothermal reservoirs.

In the present paper, the unconfined coastal aquifer with non-isothermal geothermal heating from below (Fig. 1a) is idealized as a two-dimensional porous medium bounded on the bottom by a horizontal impermeable wall and on the vertical sides by the ocean (Fig. 1b). The shape of the free surface is not known *a priori* and must be determined from the solution. The non-linear governing equations and non-linear boundary conditions are approximated by a set of linear sub-problems on the basis of perturbation analysis. Numerical results, accurate to the first-order approximation, are obtained for temperature, pressure and stream function. The effect of non-isothermal geothermal heating on the upwelling of the water table is predicted.

Governing Equations and Boundary Conditions. To simplify the mathematical formulation of the problem the following assumptions are made:

1. The flow field is steady and two-dimensional.
2. The temperature of the fluid is low corresponding to its saturated temperature for boiling to take place.
3. The Boussinesq approximation is employed; i.e., density is assumed to be constant except in the bouyancy force term.
4. There is no accretion at the free surface.
5. Fluid properties such as thermal conductivity, specific heat, kinematic viscosity, and permeability are assumed to be constant.
6. Ocean is at rest; i.e., the effects to tides are neglected.

With these approximations, the governing equations are given by

$$\text{div } \bar{v} = 0, \quad (1)$$

$$\bar{v} = -\frac{K}{\mu} (\nabla p + \rho \bar{g}), \quad (2)$$

$$\frac{\rho}{\rho_s} = 1 - \beta (T - T_s), \quad (3)$$

$$\bar{v} \cdot \nabla T = \alpha \nabla^2 T, \quad (4)$$

where \bar{v} , ρ , μ and β are the macroscopic velocity vector, density, viscosity and the thermal expansion coefficient of the fluid, p the pressure, T the temperature, g the gravitational acceleration. $\alpha = \frac{k_m}{(\rho C_p)_f}$ is the equivalent thermal diffusivity with k_m denoting the thermal conductivity of the porous medium and $(\rho C_p)_f$ the density and specific heat of the fluid. The subscript s in Eq. (3) denotes the condition in the ocean.

The boundary conditions along the ocean are given by

$$p(0, y) = p_a + \rho_s g (h - y), \quad (5)$$

$$p(l, y) = p_a + \rho_s g (h - y), \quad (6)$$

$$T(0, y) = T_s, \quad (7)$$

$$T(l, y) = T_s. \quad (8)$$

Along the impermeable surface, the boundary conditions are

$$v(x, 0) = 0, \quad (9)$$

$$T(x, 0) = T_L(x), \quad (10)$$

where $T_L(x)$ is prescribed. Along the free surface, the boundary conditions are

$$\bar{v} \cdot \bar{n}(x, \eta) = 0, \quad (11)$$

$$p(x, \eta) = P_a, \quad (12)$$

$$T(x, \eta) = T_a, \quad (13)$$

where $y = \eta(x)$ is the shape of the free surface, which is not known *a priori* and \bar{n} is the unit vector normal to the free surface, which is given by $\bar{n} = \frac{\nabla F}{|\nabla F|}$ with $F(x, y) \equiv y - \eta(x) = 0$ denoting the equation for the free surface.

With the aid of Eqs. (2) and (3), boundary condition (9) can be rewritten in terms of p to give

$$\frac{\partial p}{\partial y}(x, 0) = -\rho_s g [1 - \beta(T_L - T_s)], \quad (14)$$

whereas boundary condition Eq. (11) can be rewritten as

$$\frac{\partial \eta}{\partial x} \frac{\partial p}{\partial x}(x, \eta) - \left\{ \frac{\partial p}{\partial y}(x, \eta) + \rho_s g [1 - \beta(T_a - T_s)] \right\} = 0, \quad (15)$$

where Eq. (15) is the non-linear boundary condition at the free surface.

Since boundary conditions are now in terms of p and T , we shall eliminate u , v , ρ from Eqs. (1) through (4) and express the resultant equations in terms of p and T . Thus we have

$$\frac{\partial^2 p}{\partial x^2} + \frac{\partial^2 p}{\partial y^2} = \rho_s g \beta \frac{\partial T}{\partial y}, \quad (16)$$

$$\frac{\partial^2 T}{\partial x^2} + \frac{\partial^2 T}{\partial y^2} + \frac{K}{\mu \alpha} \left[\frac{\partial p}{\partial x} \frac{\partial T}{\partial x} + \frac{\partial p}{\partial y} \frac{\partial T}{\partial y} + \rho_s g [1 - \beta(T - T_s)] \frac{\partial T}{\partial y} \right] = 0. \quad (17)$$

We now express Eqs. (16) and (17) with boundary conditions (5) - (8), (10), (12) - (15) in dimensionless form. For this purpose we introduce the following dimensionless variables:

$$P \equiv \frac{p - p_a}{\rho_s g h}, \quad \theta \equiv \frac{T - T_s}{T_c - T_s}, \quad \bar{\eta} \equiv \frac{\eta}{h}, \quad X \equiv \frac{x}{h}, \quad Y \equiv \frac{y}{h}, \quad L \equiv \frac{l}{h}, \quad (18)$$

where T_c is the maximum temperature of the impermeable surface.

The governing equations in terms of these dimensionless variables are given by

$$\frac{\partial^2 P}{\partial X^2} + \frac{\partial^2 P}{\partial Y^2} = \epsilon \frac{\partial \theta}{\partial Y}, \quad (19)$$

and

$$\frac{\partial^2 \theta}{\partial X^2} + \frac{\partial^2 \theta}{\partial Y^2} + D \left[\frac{\partial P}{\partial X} \frac{\partial \theta}{\partial X} + \frac{\partial P}{\partial Y} \frac{\partial \theta}{\partial Y} + [1 - \epsilon \theta] \frac{\partial \theta}{\partial Y} \right] = 0, \quad (20)$$

where $\epsilon \equiv \beta(T_c - T_s)$, and $D \equiv \frac{\rho_s K g h}{\alpha \mu}$ is called the discharge number which is a measure of the imposed pressure forces to the viscous force. Boundary conditions in terms of dimensionless variables are re-arranged to give

$$P(0, Y) = 1 - Y, \quad (21a)$$

$$P(L, Y) = 1 - Y, \quad (21b)$$

$$\frac{\partial P}{\partial Y}(X, 0) = -1 + \epsilon \theta_L(X), \quad (21c)$$

$$\frac{\partial \bar{\eta}}{\partial X} \frac{\partial P}{\partial X}(X, \bar{\eta}) - \left[\frac{\partial P}{\partial Y}(X, \bar{\eta}) + 1 - \epsilon \theta_a \right] = 0, \quad (21d)$$

$$P(X, \bar{\eta}) = 0, \quad (21e)$$

$$\theta(0, Y) = 0, \quad (22a)$$

$$\theta(L, Y) = 0, \quad (22b)$$

$$\theta(X, 0) = \theta_L(X), \quad (22c)$$

$$\theta(X, \bar{\eta}) = \theta_a, \quad (22d)$$

where $\theta_a \equiv \frac{T_a - T_s}{T_c - T_s}$ and $\theta_L(X) \equiv \frac{T_L(X) - T_s}{T_c - T_s}$.

Perturbation Analysis. Since the value of ϵ in Eqs. (19) - (22) is small, we shall now obtain perturbation solution to the problem. For this purpose, we now assume that dependent variables be expanded in a power series of ϵ .

Thus, we have

$$P(X, Y) = \sum_{m=0}^{\infty} \epsilon^m P_m(X, Y), \quad (23a)$$

$$\theta(X, Y) = \sum_{m=0}^{\infty} \epsilon^m \theta_m(X, Y), \quad (23b)$$

$$\bar{\eta}(X) = 1 + \sum_{m=1}^{\infty} \epsilon^m \eta_m(X), \quad (23c)$$

where $P_m(X, Y)$, $\theta_m(X, Y)$ and $\eta_m(X)$ are perturbation functions to be determined. Substituting Eqs. (23) into Eqs. (19) - (22), making a Taylor's series expansion on boundary conditions (21d), (21e), and (22d), and collecting terms of like power in ϵ , we have the following set of sub-problems.

Zero-Order Approximations

The zero-order problem for P is given by

$$\frac{\partial^2 P_0}{\partial X^2} + \frac{\partial^2 P_0}{\partial Y^2} = 0, \quad (24)$$

with boundary conditions given by

$$P_0(0, Y) = 1 - Y, \quad (25a)$$

$$P_0(L, Y) = 1 - Y, \quad (25b)$$

$$\frac{\partial P_0}{\partial Y}(X, 0) = -1, \quad (25c)$$

$$P_0(X, 1) = 0. \quad (25d)$$

Solution to the zero-order problem for P is obviously given by

$$P_0(X, Y) = 1 - Y, \quad (26)$$

which physically means the hydrostatic situation.

With the aid of Eq. (26), the zero-order problem for θ is given by

$$\frac{\partial^2 \theta_0}{\partial X^2} + \frac{\partial^2 \theta_0}{\partial Y^2} = 0, \quad (27)$$

with boundary conditions given by

$$\theta_0(0, Y) = 0, \quad (28a)$$

$$\theta_0(L, Y) = 0, \quad (28b)$$

$$\theta_0(X, 1) = \theta_a, \quad (28c)$$

$$\theta_0(X, 0) = \theta_L(X). \quad (28d)$$

Thus, to the zero-order approximation, pressure is given by the hydrostatic pressure and temperature distribution is due to heat conduction; the fluid flow and heat transfer are decoupled in the zero-order approximation. Furthermore, Eqs. (25d) and (28c) show that we have successfully transferred the boundary conditions at the unknown free surface to $Y = 1$.

First-Order Approximations

With the aid of Eq. (26), the first order problem for P is given by

$$\frac{\partial^2 P_1}{\partial X^2} + \frac{\partial^2 P_1}{\partial Y^2} = \frac{\partial \theta_0}{\partial Y}, \quad (29)$$

where the right hand side of Eq. (29) is known from the zero-order problem.

The boundary conditions for P_1 are given by

$$P_1(0, Y) = 0, \quad (30a)$$

$$P_1(L, Y) = 0, \quad (30b)$$

$$\frac{\partial P_1}{\partial Y}(X, 1) = \theta_a, \quad (30c)$$

$$\frac{\partial P_1}{\partial Y}(X, 0) = \theta_L(X). \quad (30d)$$

Once P_1 is determined, $\eta_1(X)$ is obtained from

$$\eta_1(X) = P_1(X, 1), \quad (30e)$$

which follows from substituting Eqs. (23a) and (23c) into boundary condition (21e) and making a Taylor series expansion. Eq. (30e) gives the influence of

the geothermal heating on the shape of the free surface. Eqs. (29) - (30) show that the value of P_1 , and consequently $\bar{\eta}_1$, depends on the vertical temperature gradient in the medium as well as the prescribed temperature distribution on the impermeable surface. Thus, to the first-order approximation, the amount of upwelling of water table, which is given by $\epsilon\eta_1$, depends entirely on the amount of geothermal heating.

With the aid of Eq. (26), the first-order approximation for θ is

$$\frac{\partial^2 \theta_1}{\partial X^2} + \frac{\partial^2 \theta_1}{\partial Y^2} = -D \left[\frac{\partial P_1}{\partial X} \frac{\partial \theta_0}{\partial X} + \frac{\partial P_1}{\partial Y} \frac{\partial \theta_0}{\partial Y} - \theta_0 \frac{\partial \theta_0}{\partial Y} \right], \quad (31)$$

with boundary conditions given by

$$\theta_1(0, Y) = 0, \quad (32a)$$

$$\theta_1(L, Y) = 0, \quad (32b)$$

$$\theta_1(X, 0) = 0, \quad (32c)$$

$$\theta_1(X, 1) = -P_1(X, 1) \frac{\partial \theta_0}{\partial Y}(X, 1). \quad (32d)$$

An alternate formulation in terms of stream function is shown in Appendix A.

The governing equations for the zero-order and the first-order problems as given by Eqs. (27) - (32) are respectively the Laplace equation and Poisson equation with nonhomogeneous boundary conditions. In principle they can be solved in closed form by the classical method of separation of variables. However, the numerical evaluation of the resultant expressions in terms of many double and triple Fourier series will be of dubious value because of its slow

convergent rate. For this reason we resort to the numerical solution of these linear problems by the finite difference method.

Numerical Computations and Results. The standard five point formula of the finite difference method is applied to Eqs. (27), (29), and (31). The resultant linear algebraic equations, as given in Appendix B, are solved by the Gauss-Seidel iteration method. The mesh size in both X and Y directions is chosen to be 0.1. The iteration process is terminated when the maximum value is changed by less than 0.1% of the previous cycle. Computation begins with the determination of θ_0 from Eqs. (B-12) - (B-16). After values of θ_0 at all grid points are obtained, the partial differentiation of θ_0 is computed by using the IBM scientific subroutine DET5. The partial derivatives of θ_0 are then stored on disk and will be used for the determination of P_1 and ψ_1 from Eqs. (B-17) - (B-30) and Eqs. (B-50) - (B-52). The differentiation of P_1 and the determination of θ_1 from Eqs. (B-38) - (B-42) are done in the same manner.

The parameters for the present problem are L the aspect ratio, D the discharge number, and ϵ the perturbation parameter. Grid values of pressure, temperature, and stream function are computed for L=4, $\epsilon=0.1$ with D=50, and 500 for the following three temperature distributions of the impermeable surface:

$$(1) \quad \theta_L = \exp \left[-\left(\frac{X - 2.0}{0.5}\right)^2 \right], \text{ with a maximum temperature at } X=2.0,$$

$$(2) \quad \theta_L = \exp \left[-\left(\frac{X - 0.5}{0.5}\right)^2 \right], \text{ with a maximum temperature at } X=0.5,$$

$$(3) \quad \theta_L = \exp \left[-\left(\frac{X - 0.5}{0.1}\right)^2 \right], \text{ with a maximum temperature at } X=0.5.$$

Comparison of the numerical results for Cases 1 and 2 will show the effect of the location of heat source whereas the comparison of results for Case 2 (a broad heat source) and Case 3 (a narrow heat source) will show the effect of the size of the heat source.

Fig. 2 shows the contour of the first order perturbation of stream function, ψ_1 , for Case 1. As is shown in the figure, the fluid particles begin to rise as they approach the point of maximum surface temperature. This is because the density of the fluid becomes smaller as its temperature rises. As the fluid particles rise to a colder region they begin to lose heat and will begin their descending paths when the density becomes the same as that of the surrounding fluid. Since $\psi_0 = 0$ and $\psi = \epsilon\psi_1$ to the first order approximation, the amount of convective current can be estimated by the difference in the values of the stream function $\epsilon\psi_1$. It is worth mentioning that, to the first order approximation, the movement of fluid particles is induced by the horizontal temperature gradient by conduction as shown in Eq. (A-17) in Appendix A. The value of the stream function is therefore independent of D and is proportional to ϵ .

Fig. 3a shows the contours of the first-order pressure function P_1 for Case 1. As is shown in Eqs. (29) - (30), P_1 is induced by the non-isothermal temperature distribution on the boundary and the vertical temperature gradient. The value of P_1 is independent of D , with a negative value in the lower portion of the aquifer and a minimum value at the point of maximum surface temperature. On the other hand the values of P_1 is positive in the upper portion of the aquifer with a maximum value at the point (2,1). Thus the fluid particles are drawn inward in the lower portion of the aquifer and are forced to move toward the ocean in the upper portion of the aquifer. Fig. 3b shows the pressure

contours for Case 1 with $\varepsilon = 0.1$ and for all values of D . The fact that the pressure contours are almost horizontal indicates that the pressure in an unconfined geothermal reservoir can be approximated by hydrostatic pressure.

Fig. 4a shows the contours of the zero-order perturbation function for temperature for Case 1. In the zero-order approximation, heat is transferred by conduction, as a result of non-isothermal temperature on the boundary. Thus the value of θ_0 is independent of D . Fig. 4b shows the contours of first-order perturbation temperature θ_1 , the temperature correction due to convective current. As is expected, the convective current helps to diffuse heat, and consequently, the contours of temperature are pushed further away from the heat source as the value of D is increased. The maximum value of θ_1 is in a region that is slightly above the point of maximum geothermal heating. The regions of negative value of θ_1 indicate the inward movement of cold water from the ocean. The effect of discharge number on temperature contours for $\varepsilon = 0.1$ is shown in Fig. 4c. Comparison of Figs. 4a and 4c shows that the difference between temperature contours θ_0 and θ_1 is small for $D = 50$, indicating that heat transfer by conduction is predominant for small value of D . There is significant difference in temperature contours for $D = 500$ especially in the region of maximum heating, which suggests that there is a strong convection current there.

The effects of discharge number, the location of the heat source and the size of the heat source on the horizontal temperature distribution are shown in Figs. 5a, 5b, and 5c. The prescribed temperature distribution of the impermeable rock is indicated by $Y = 0$. It is interesting to note that, with the exception of narrow heat source, the width of the temperature profiles at lower elevations fall within the temperature profile at $Y = 0$, indicating that the lateral diffusion of heat by convection is not very effective. As is expected, temperature is higher for higher values of D at the same location (Fig. 5a). To show

the effect of location on the horizontal temperature distribution, results for Cases 1 and 2 with $D = 500$ and $\epsilon = 0.1$ are plotted in Fig. 5b. When the heat source is near the ocean as in Case 2, although there is a significant drop in temperature on the ocean side of the heat source due to inward movement of cold sea water, temperature on the other side of the heat source is only slightly affected. To show the effect of size of the heat source on the horizontal temperature distribution, results for Case 2 (a broad heat source) and Case 3 (a narrow heat source) with $D = 500$ and $\epsilon = 0.1$ are plotted in Fig. 5c. It is shown in this figure that temperature is higher for a broad heat source than that of a narrow heat source.

The effect of discharge number on vertical temperature profiles is shown in Fig. 6a (Case 1) and in Fig. 6b (Case 2). For locations directly above the point of maximum surface temperature (i.e., at $X = 2$ in Fig. 6a and $X = 0.5$ in Fig. 6b), temperature is higher for higher value of D . Similar behavior exists in the upper portion of the aquifer. However, in the lower portion of the aquifer, temperature decreases as the value of D is increased. This is due to the inflow of colder seawater in the lower portion of the aquifer and the outflow of warmer seawater in the upper portion of the aquifer. The behavior is more pronounced for Case 2 (Fig. 6b) than Case 1 (Fig. 6a) since the amount of inflow of cold seawater is larger for Case 2. To show the effect of location of the heat source on vertical temperature profiles, data for Figs. 6a and 6b with $D = 500$ and $\epsilon = 0.1$ are replotted in Fig. 6c. It is shown that the effect of location on vertical temperature profiles is small for position directly above the point of maximum surface temperature ($X = 2$ and $X = 0.5$). For the vertical positions 0.4 unit away from the point of maximum surface temperature, comparison of the curve of $X = 1.6$ for Case 1 to that of $X = 0.1$ for Case 2

shows that there is a significant drop in temperature at the ocean side of the heat source. Similar comparison of the curves $X = 2.4$ (for Case 1) and $X = 0.9$ (for Case 2) indicates that the temperature drop is small at the other side of the heat source. The effect of the size of the heat source on vertical temperature profiles for $D = 500$ and $\epsilon = 0.1$ is shown in Fig. 6d. It is shown that there is a significant drop in temperature if the size of the heat source decreases.

Figs. 7a and 7b show the effect of location and the size of heat source on η_1 , the first-order perturbation function for the shape of water table. To the first-order approximation the upwelling of water table is given by $\epsilon\eta_1$, and is independent of D . The amount of upwelling depends on the vertical temperature gradient of the porous medium and the temperature distribution of the impermeable surface. The size and the location of the heat source have a strong influence on the amount of upwelling of water table. The maximum value of η_1 is approximately 0.08 at $X = 2$ for Case 1 (Fig. 7a). For a heat source near the ocean (Fig. 7b), it is interesting to note that the location of maximum water table height is not necessarily located directly above the point of maximum temperature of the impermeable surface. In fact, the position of maximum value of η_1 moves inland as the size of the heat source is increased.

Concluding Remarks. A parametric study has been conducted to investigate the effects of various parameters on the movement of seawater, the upwelling of water table, the pressure and temperature distributions in a geothermal reservoir. It has been found, to the first-order approximation, that (1) the pressure in the unconfined geothermal reservoir is almost hydrostatic, (2) the flow rate of sea water depends only on the horizontal temperature gradient of

the reservoir, (3) although there is some decrease in temperature distribution in the lower portion of the aquifer in a small region near the ocean as a result of inflow of cold water, the water also acts as a heat-carrier in the rest of aquifer, (4) the convection of heat is more efficient vertically than horizontally, (5) the size of the geothermal source has an important effect on the temperature distribution in the reservoir, (6) the location of the heat source will have some effect on the temperature distribution in the region near the ocean, its effect on temperature at the rest of aquifer is small, (7) the discharge number has a strong effect on temperature distribution in the aquifer, and (8) there is a noticeable upwelling of water table at the location directly above the heat source; the amount of upwelling depends on the vertical temperature gradient of the porous medium and the prescribed temperature of the impermeable surface. The upwelling of water table as a result of geothermal heating is predicted analytically for the first time.

The perturbation method is used in the present analysis. The major advantages of the application of the method to the present problem are (1) the problem becomes linear and the difficulty in the non-convergence of iteration associated with the numerical solution of non-linear finite difference equations does not exist, (2) the unknown position of the water table is explicitly determined from the first-order problem, thus the usual practice of the iteration of position of water table is avoided, and (3) a clearer physical picture emerged with regard to the driving forces and the role played by various parameters in heat transfer and fluid flow characteristics in a geothermal reservoir.

Acknowledgment. The authors wish to thank Professor H. J. Ramey, Jr., of Stanford University for suggesting the problem and his encouragement throughout this work. Thanks are also due to Professors P. C. Yuen, B. H. Chen, L. S. Lau, W. Brigham, and Mr. J. F. Mink for helpful discussion and to Mr. G. Nishiura for assistance in the numerical computation. This work was supported by the RANN Directorate, National Science Foundation under Grant No. GI-38319.

REFERENCES

- Bories, S. A. and M. A. Combarous, Natural Convection in a Sloping Porous Layer, *Journal of Fluid Mechanics*, 57, 63-70, 1973.
- Chan, B. K. C., C. M. Ivey, and J. M. Barry, Natural Convection in Enclosed Porous Media with Rectangular Boundaries, *Journal of Heat Transfer*, 21-27, Feb. 1970.
- Combarous, M. A. and P. Bia, Combined Free and Forced Convection in Porous Media, *Soc. Petroleum Engineering Journal*, 399-405, 1971.
- Donaldson, I. G., Temperature Gradients in the Upper Layers of the Earth's Crust Due to Convective Water Flows, *Journal of Geophysical Research*, 67, 3449-3459, 1962.
- Elder, J. W., Steady Free Convection in a Porous Medium Heated from Below, *Journal of Fluid Mechanics*, 27, 29-48, 1967.
- Elder, J. W., Transient Convection in a Porous Medium, *Journal of Fluid Mechanics*, 27, 609-623, 1967.
- Henry, H. R. and F. A. Kohout, Circulation Patterns of Saline Groundwater Affected by Geothermal Heating--As Related to Waste Disposal, *Underground Waste Management and Environmental Implications*, 18, 202-221, 1973.
- Holst, P. H. and K. Aziz, A Theoretical and Experimental Study of Natural Convection in a Confined Porous Medium, *Canadian Journal of Chemical Engineering*, 50, 232-241, 1972.
- Holst, P. H. and K. Aziz, Transient Three-Dimensional Natural Convection in Confined Porous Media, *Int. J. Heat Mass Transfer*, 15, 73-90, 1972.
- Horton, C. W. and F. T. Rogers, Jr., Convective Currents in a Porous Medium, *Journal of Applied Physics*, 16, 367-370, 1945.
- Katto, Y. and T. Masuoka, Criterion for the Onset of Convective Flow in a Fluid in a Porous Medium, *Int. J. Heat Mass Transfer*, 10, 297-309, 1967.
- Keller, G. V., Research Drilling at the Summit of Kilauea Volcano, presented at U.S.-Japan Cooperative Science Seminar on "The Utilization of Volcano Energy," Hilo, Hawaii, Feb. 4-8, 1974.
- Lapwood, E. R., Convective of a Fluid in a Porous Medium, *Proc., Cambridge Phil. Soc.*, 44, 508-521, 1948.
- Prats, M., The Effect of Horizontal Fluid Flow in Thermally Induced Convection Currents in Porous Media, *Journal of Geophysical Research*, 71, 4835-4838, 1966.
- Wooding, R. A., Steady State Free Thermal Convection of Liquid in a Saturated Permeable Medium, *Journal of Fluid Mechanics*, 2, 273-285, 1957.
- Wooding, R. A., Rayleigh Instability of a Thermal Boundary Layer in Flow Through a Porous Medium, *Journal of Fluid Mechanics*, 183-192, 1961.

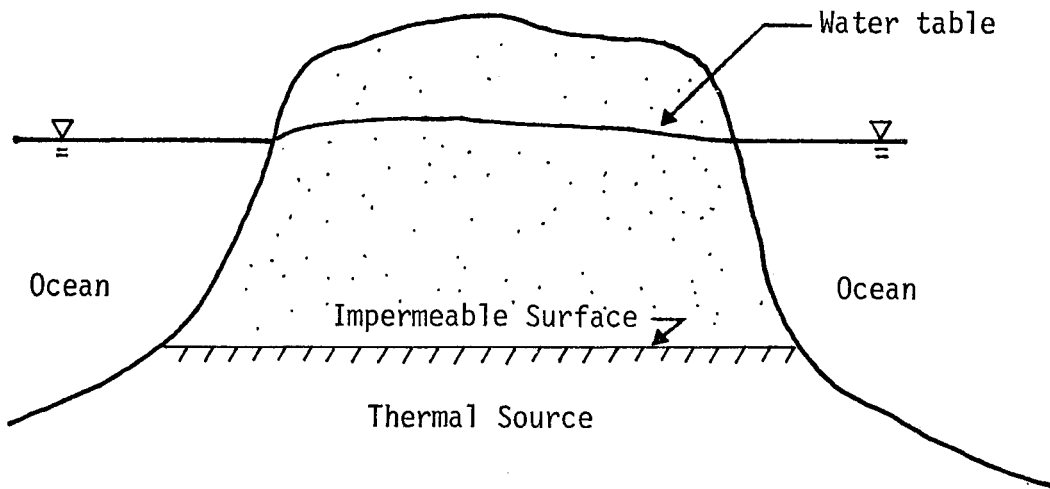


FIG. 1A. COASTAL UNCONFINED AQUIFER WITH THERMAL SOURCE

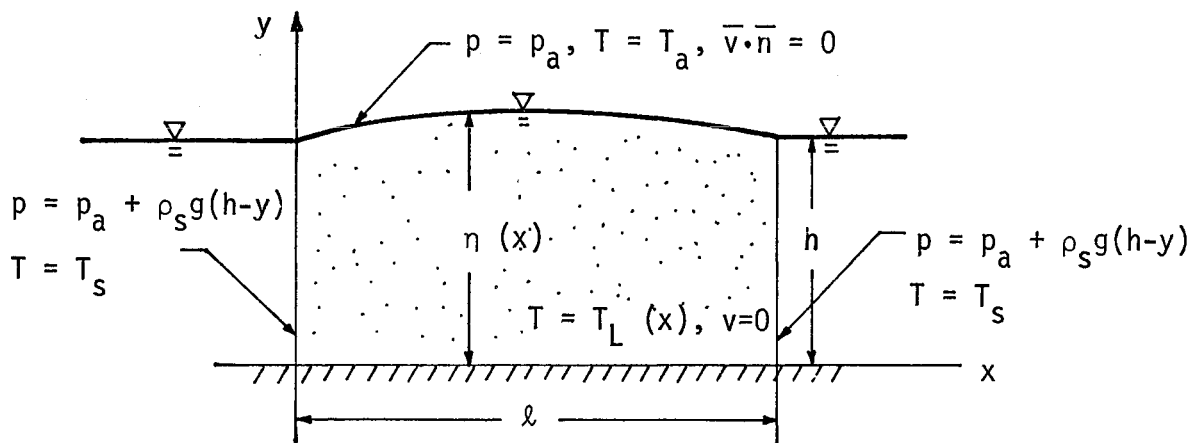


FIG. 1B. RECTANGULAR MODEL OF AQUIFER

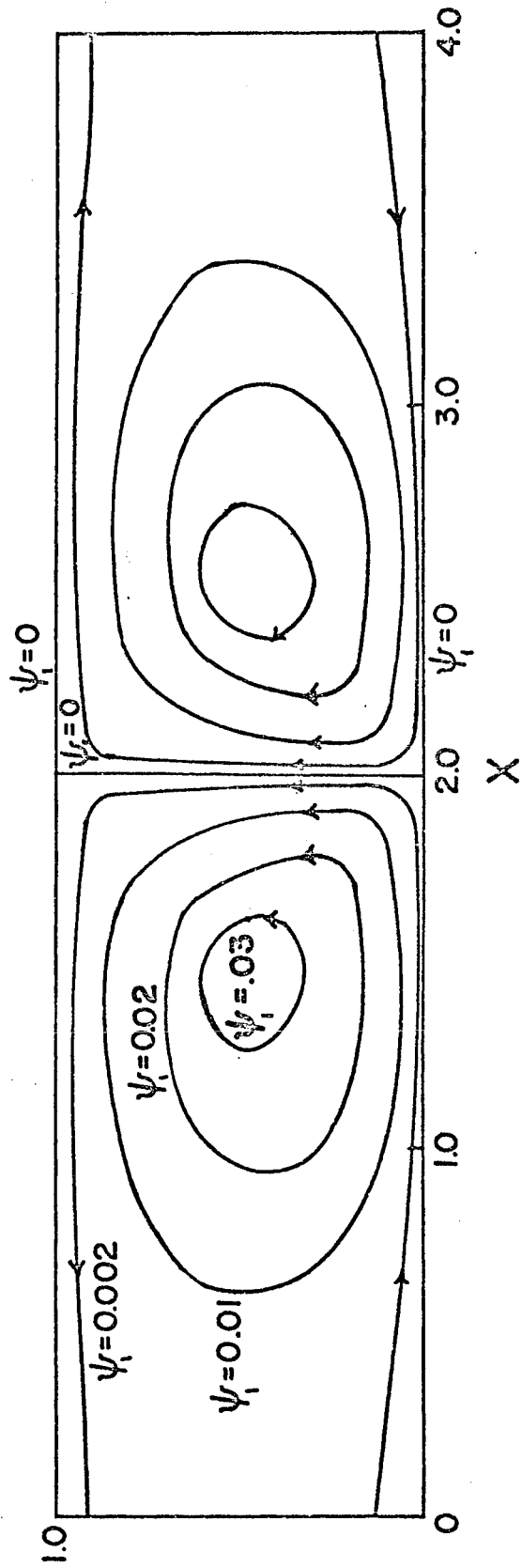


FIG. 2. CONTOURS OF FIRST-ORDER PERTURBATION FOR STREAM FUNCTION

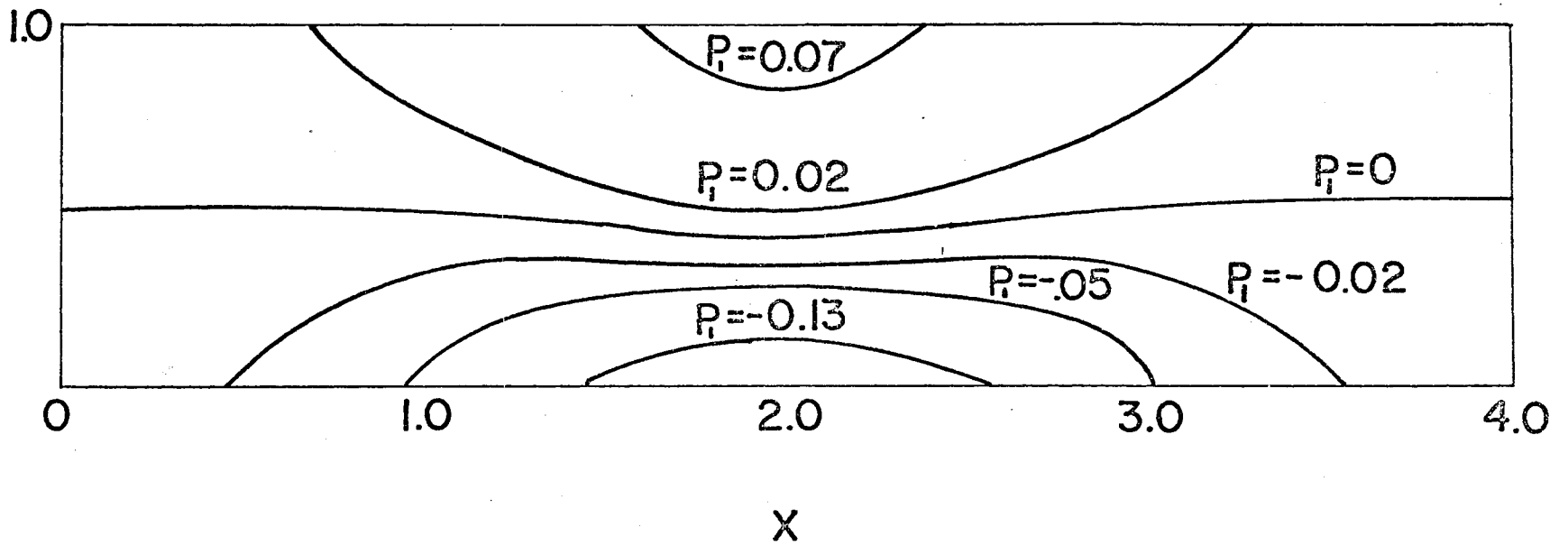


FIG. 3A. CONTOURS OF FIRST-ORDER PERTURBATION FUNCTION FOR PRESSURE

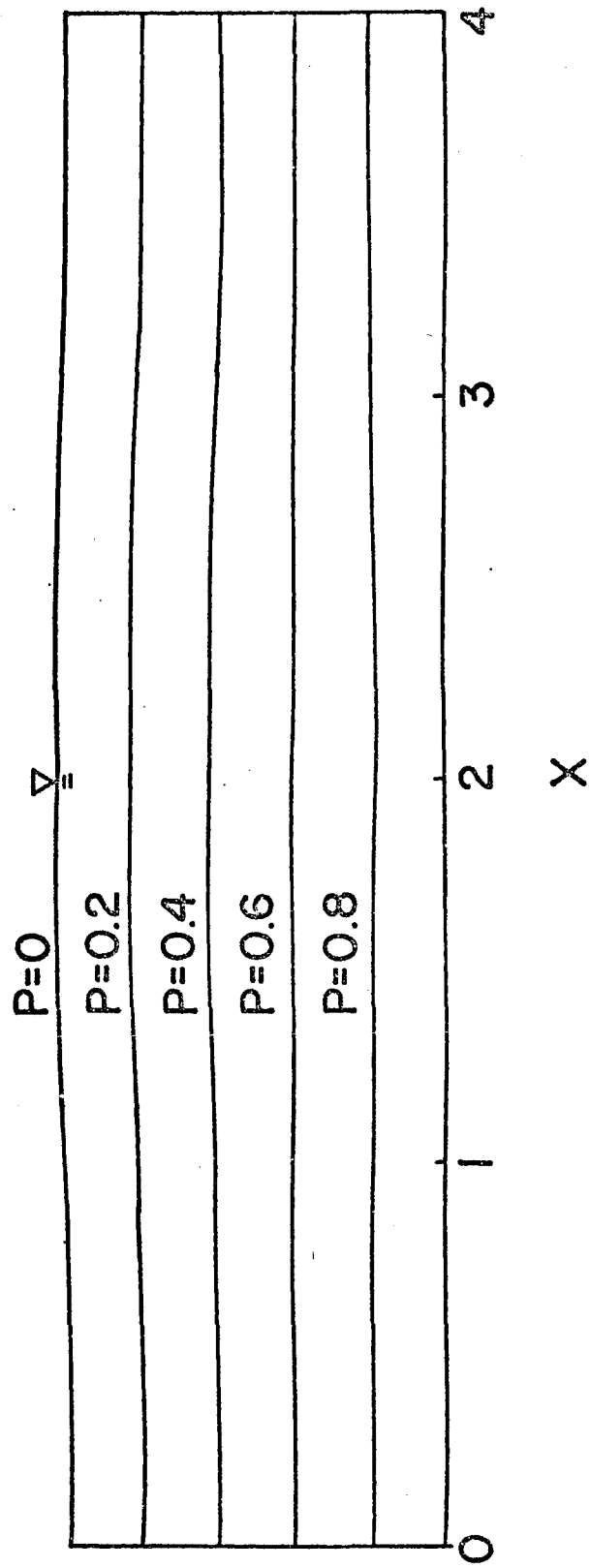


FIG. 3B. PRESSURE CONTOURS FOR CASE 1

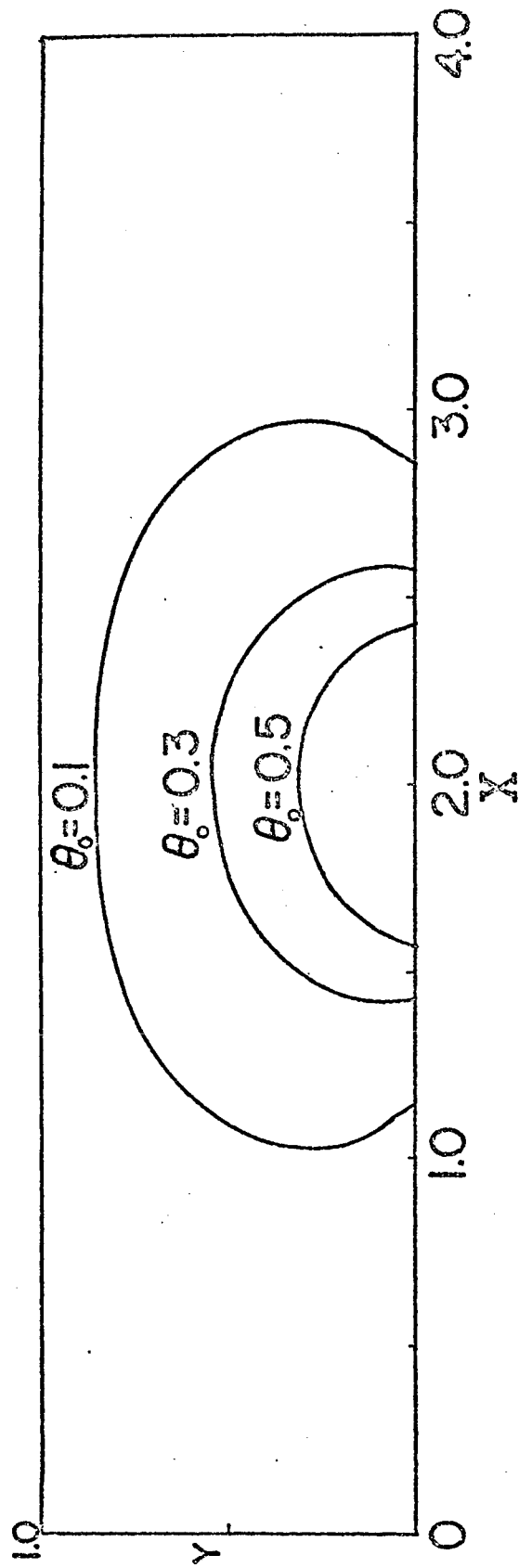


FIG. 4A. CONTOURS OF ZERO-ORDER PERTURBATION FUNCTION FOR TEMPERATURE

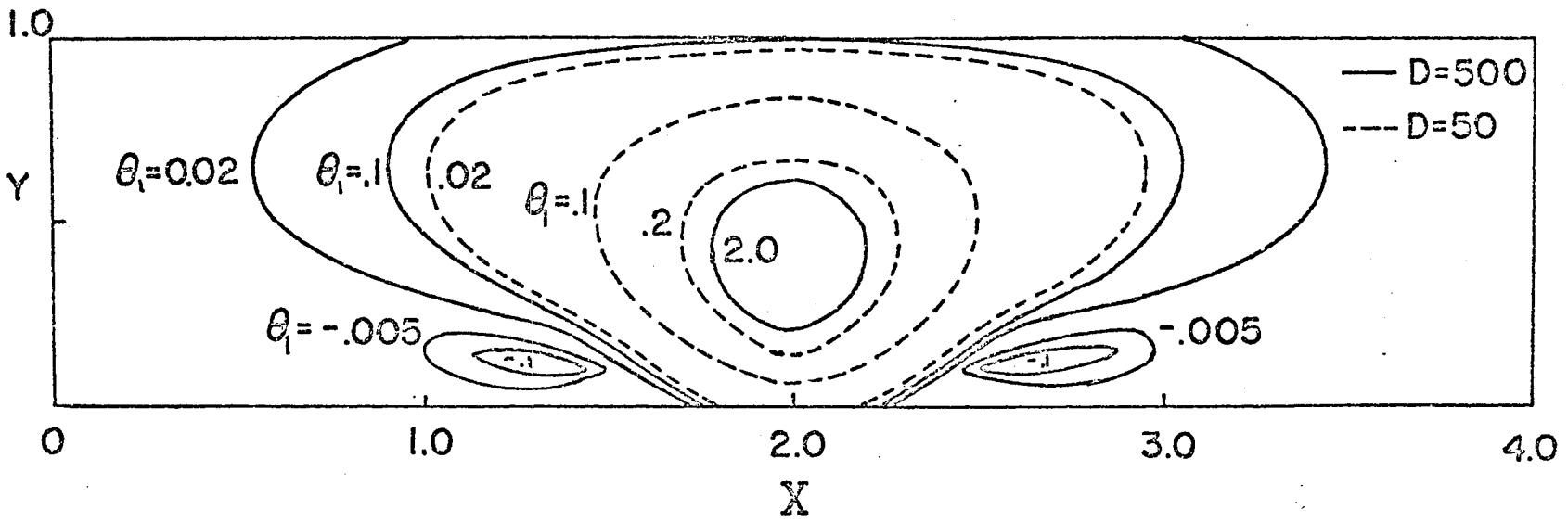


FIG. 4B. EFFECT OF DISCHARGE NUMBER ON THE CONTOURS OF FIRST-ORDER PERTURBATION FUNCTION OF TEMPERATURE

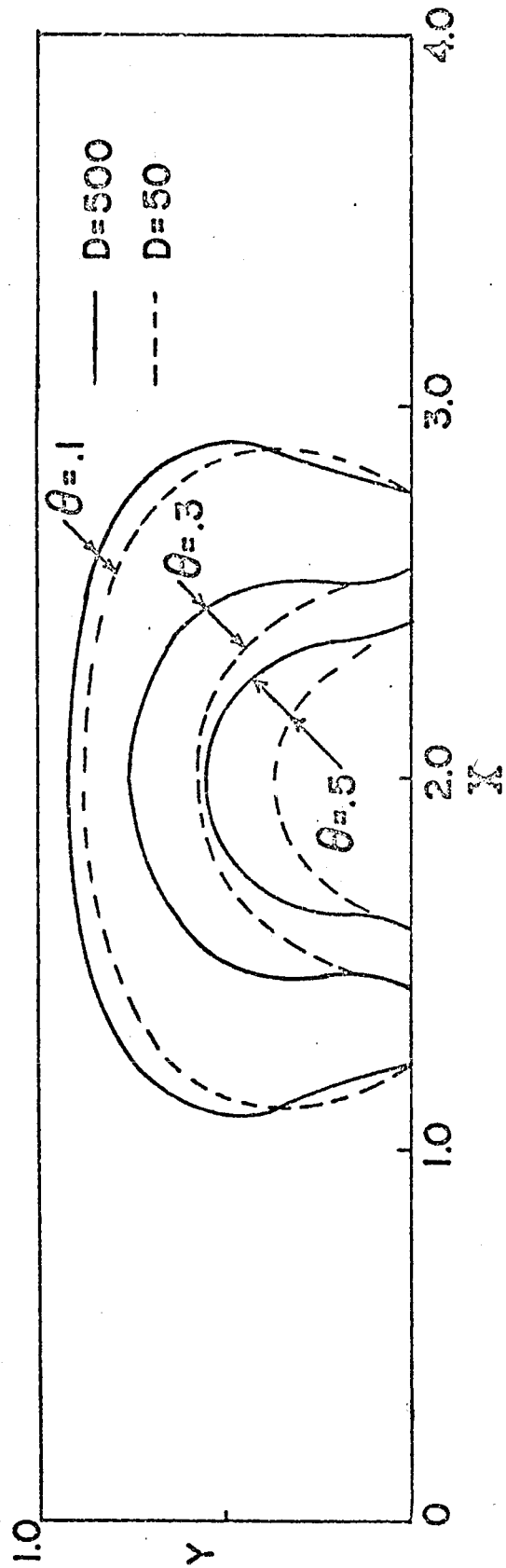


FIG. 4c. EFFECT OF DISCHARGE NUMBER ON TEMPERATURE CONTOURS FOR CASE 1

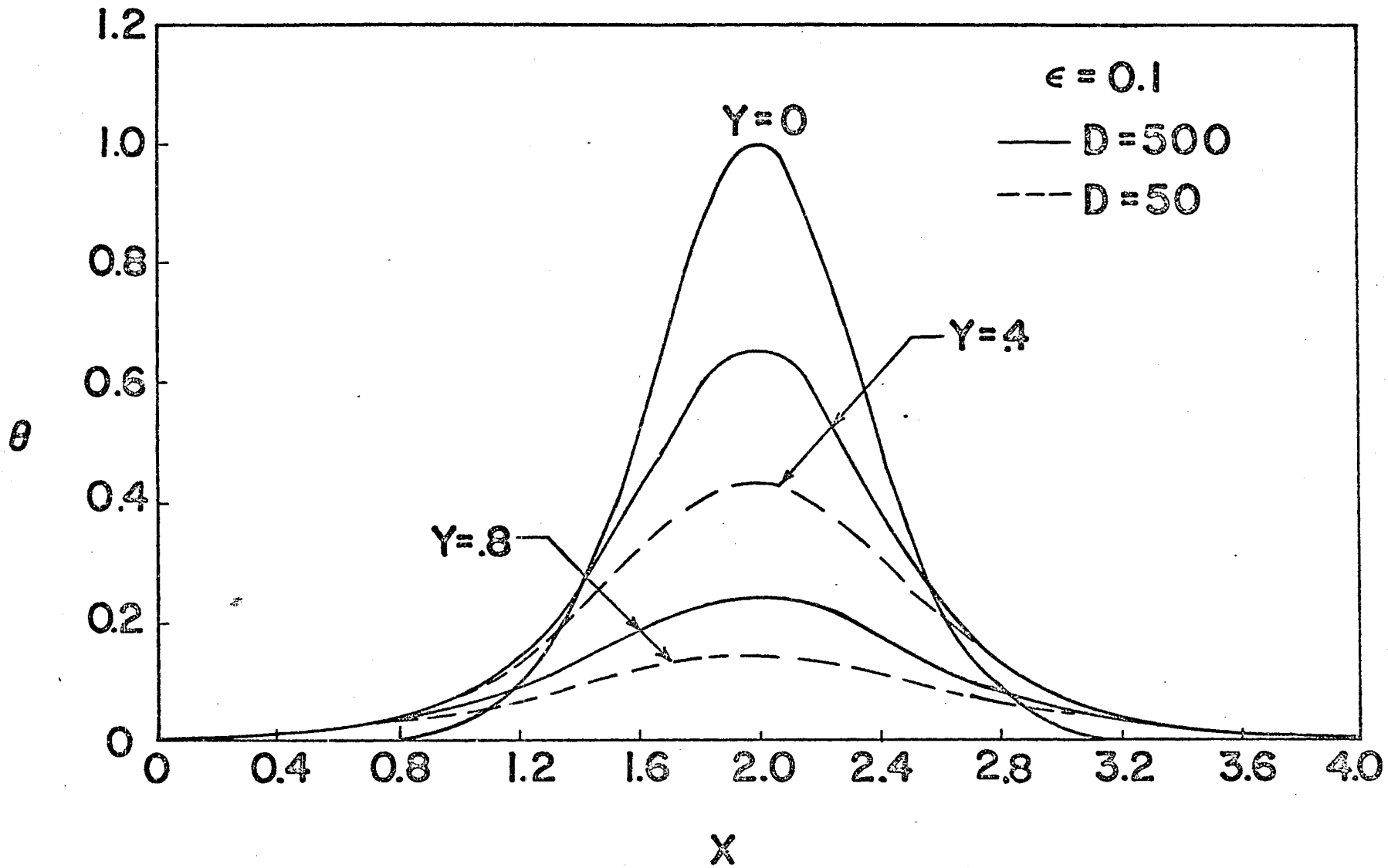


FIG. 5A. EFFECT OF DISCHARGE NUMBER ON THE HORIZONTAL TEMPERATURE DISTRIBUTION FOR CASE 1

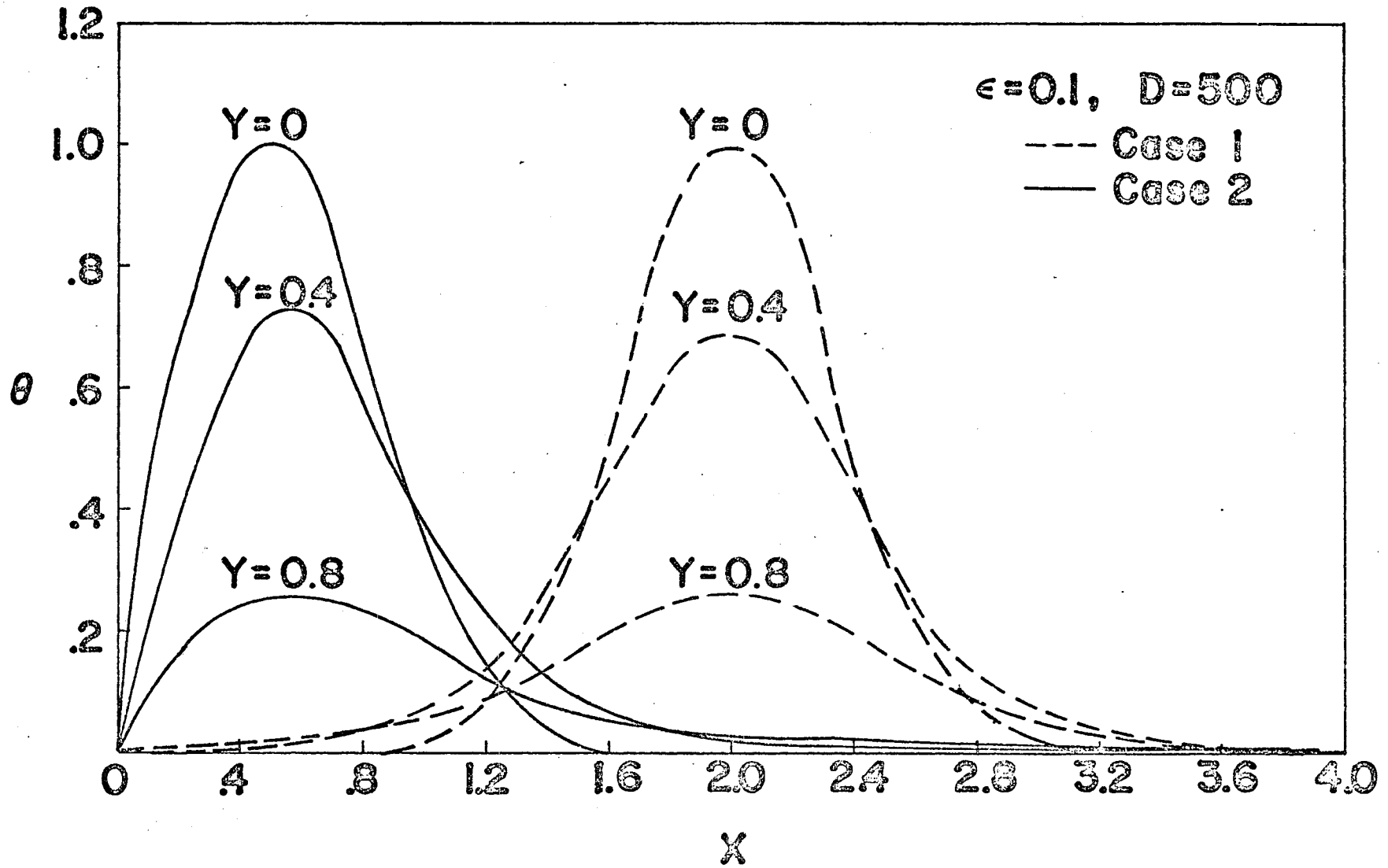


FIG. 5B. EFFECT OF THE LOCATION OF HEAT SOURCE ON THE HORIZONTAL TEMPERATURE DISTRIBUTION

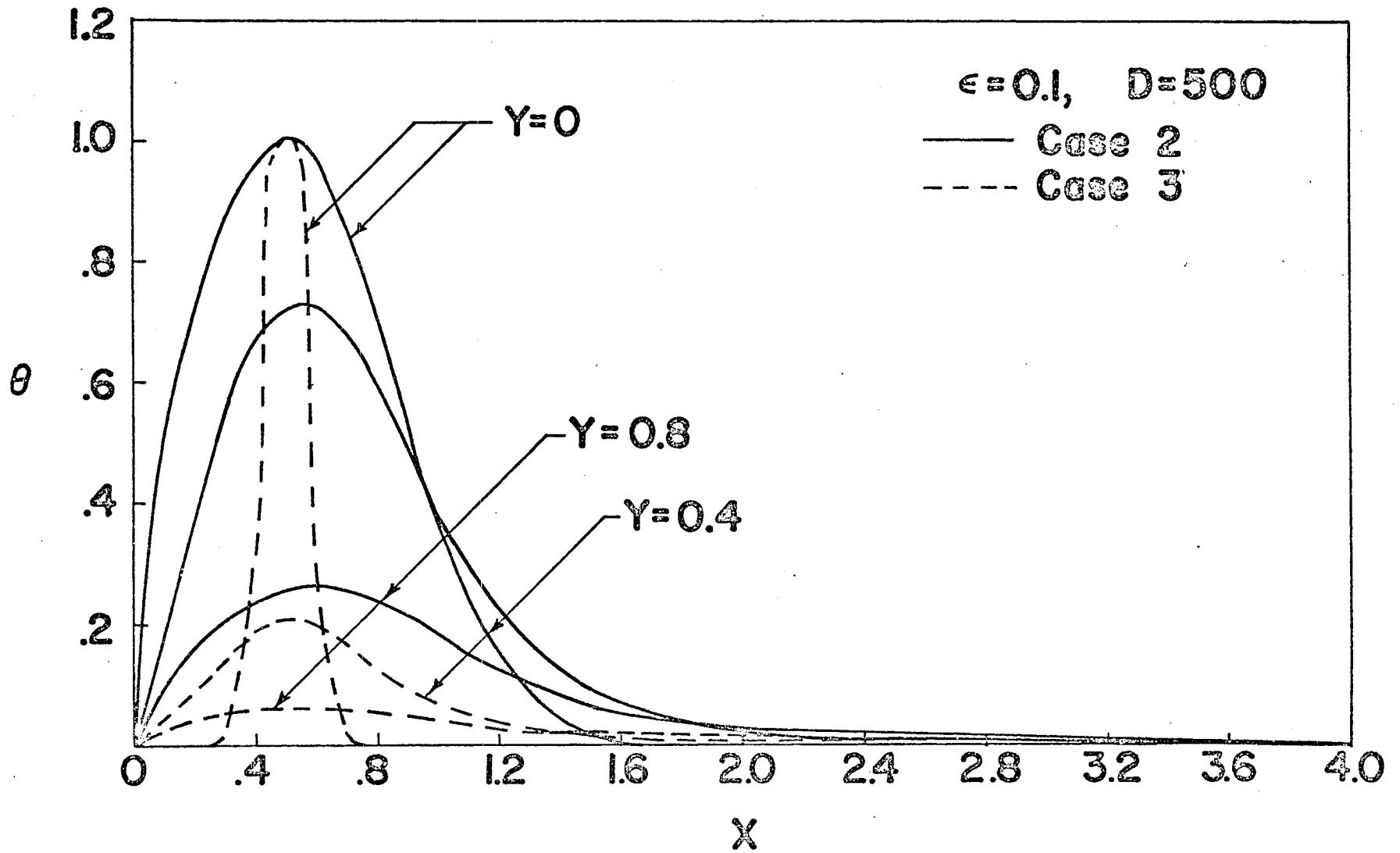


FIG. 5c. EFFECT OF THE SIZE OF THE HEAT SOURCE ON THE HORIZONTAL TEMPERATURE DISTRIBUTION

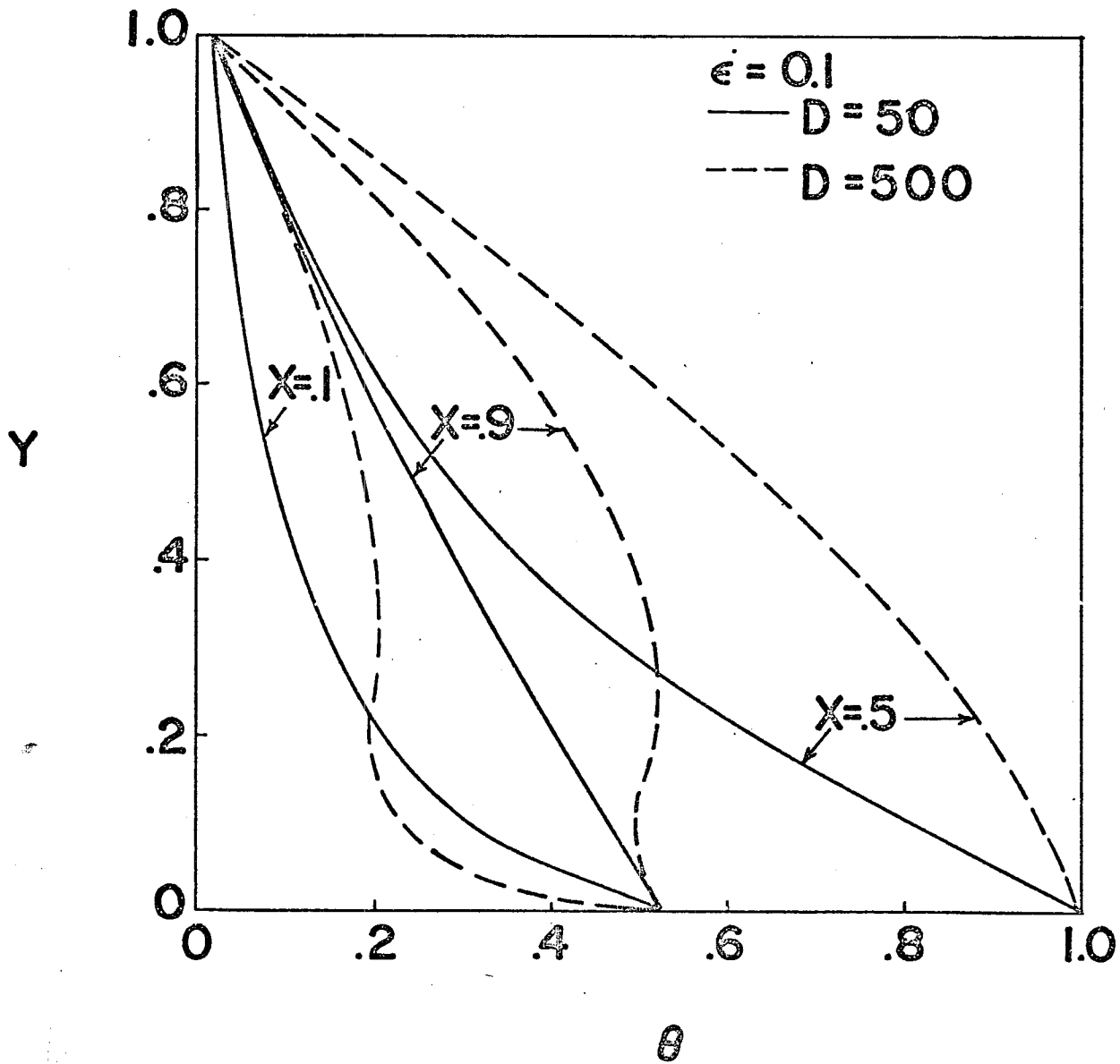


FIG. 6A. EFFECT OF DISCHARGE NUMBER ON THE VERTICAL TEMPERATURE PROFILE FOR CASE 1

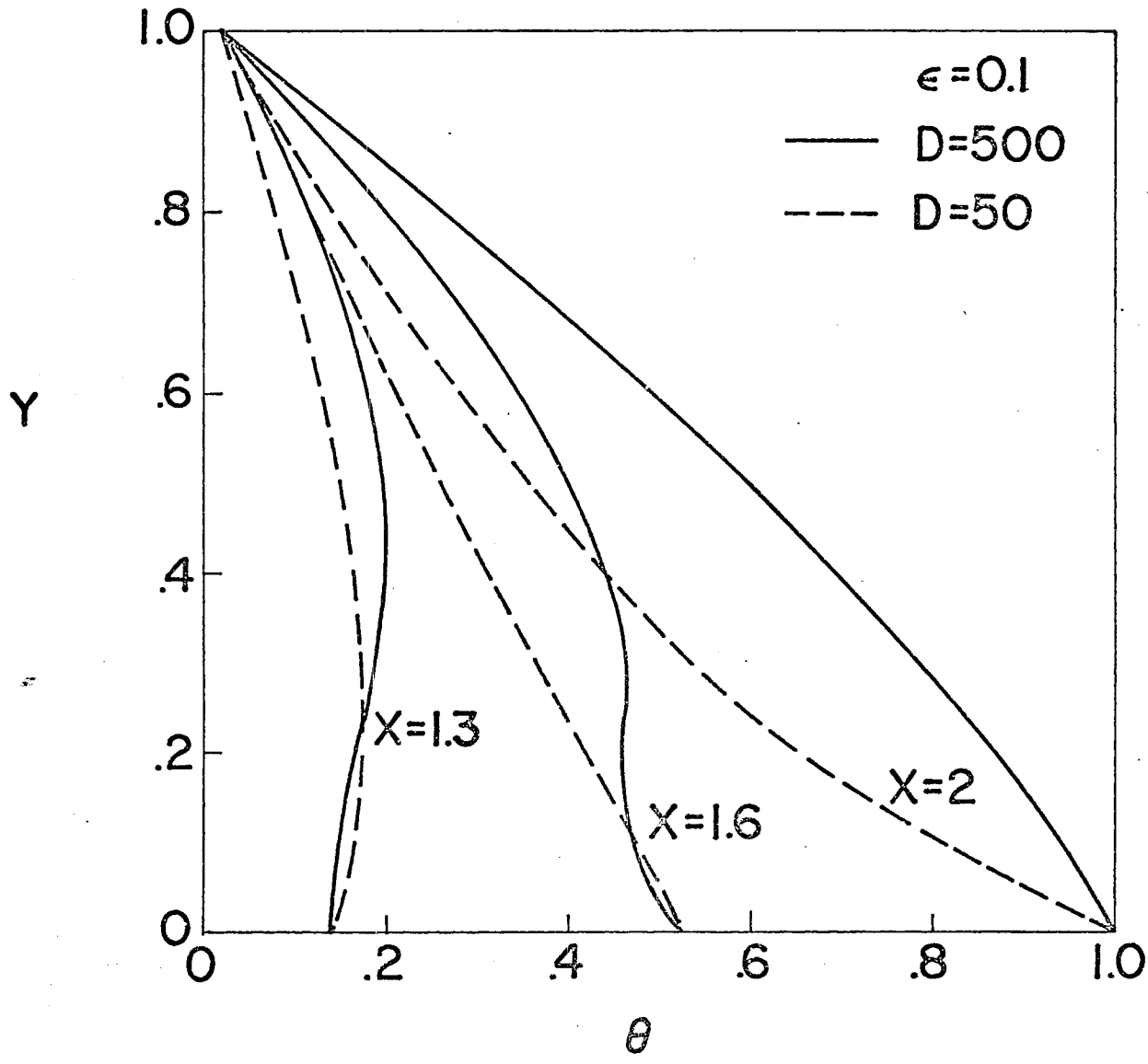


FIG. 6B. EFFECT OF DISCHARGE NUMBER ON VERTICAL TEMPERATURE PROFILES FOR CASE 2

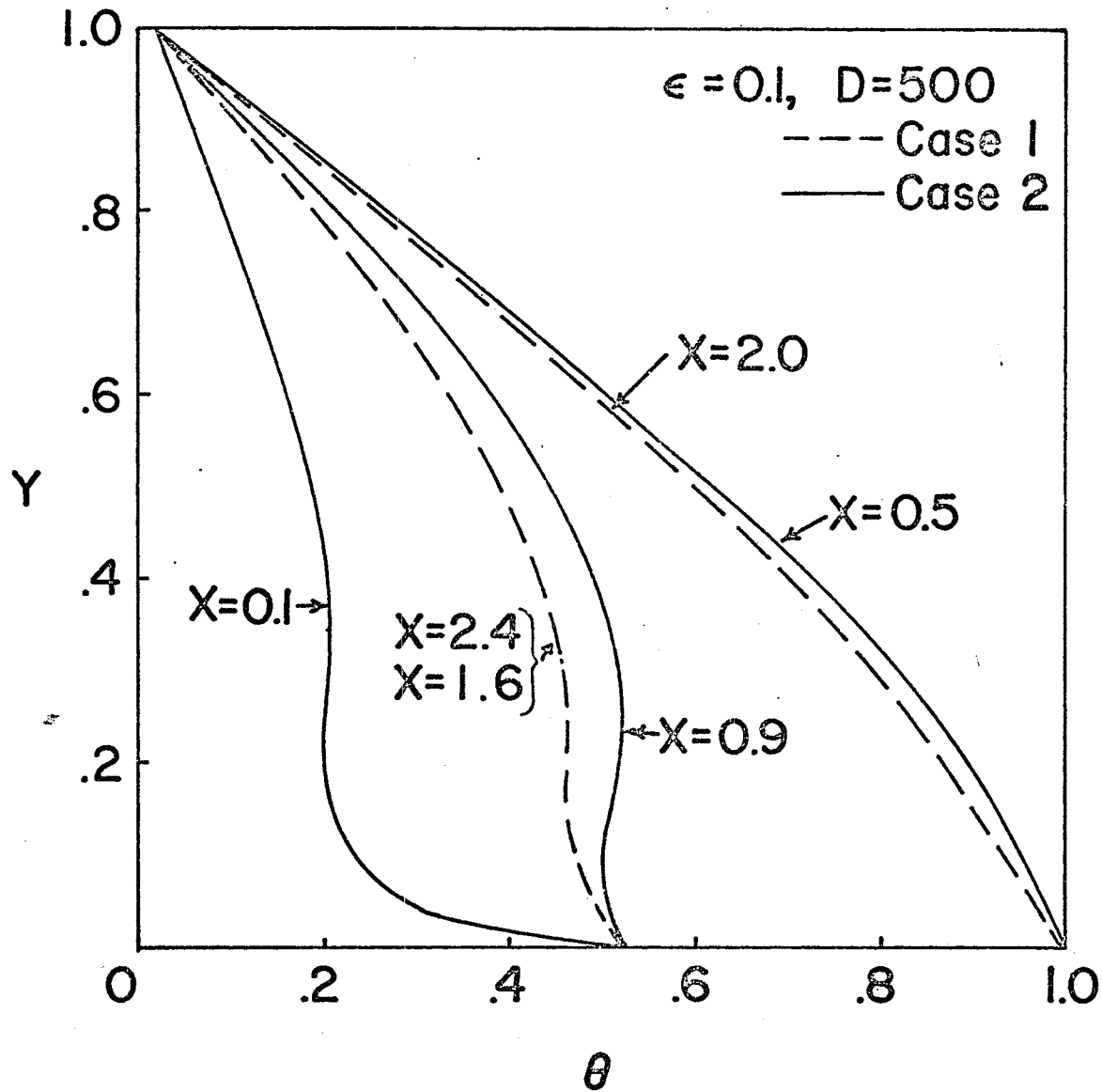


FIG. 6C. EFFECT OF THE LOCATION OF THE HEAT SOURCE ON VERTICAL TEMPERATURE PROFILES

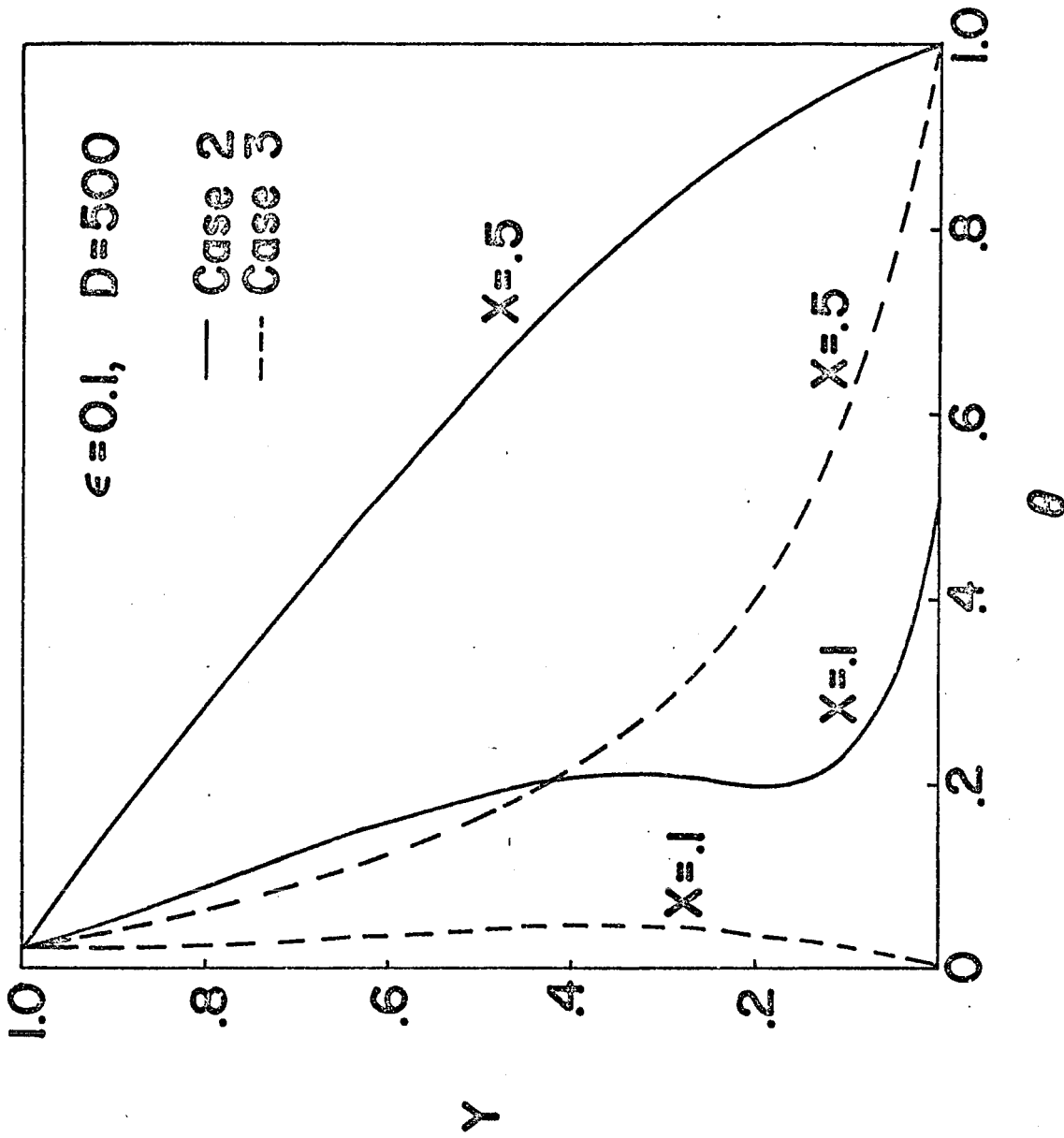


FIG. 6D. EFFECT OF THE SIZE OF THE HEAT SOURCE ON VERTICAL TEMPERATURE PROFILES

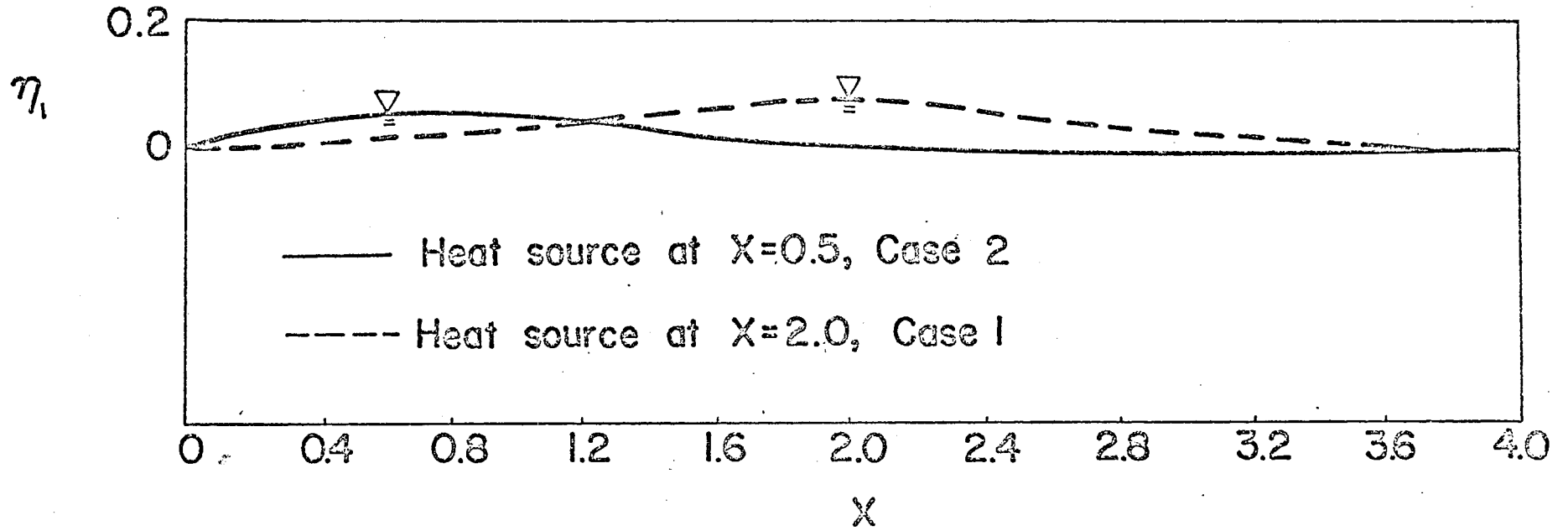


FIG. 7A. EFFECT OF THE LOCATION OF THE HEAT SOURCE ON THE FIRST-ORDER PERTURBATION FUNCTION FOR THE UPWELLING OF WATER TABLE

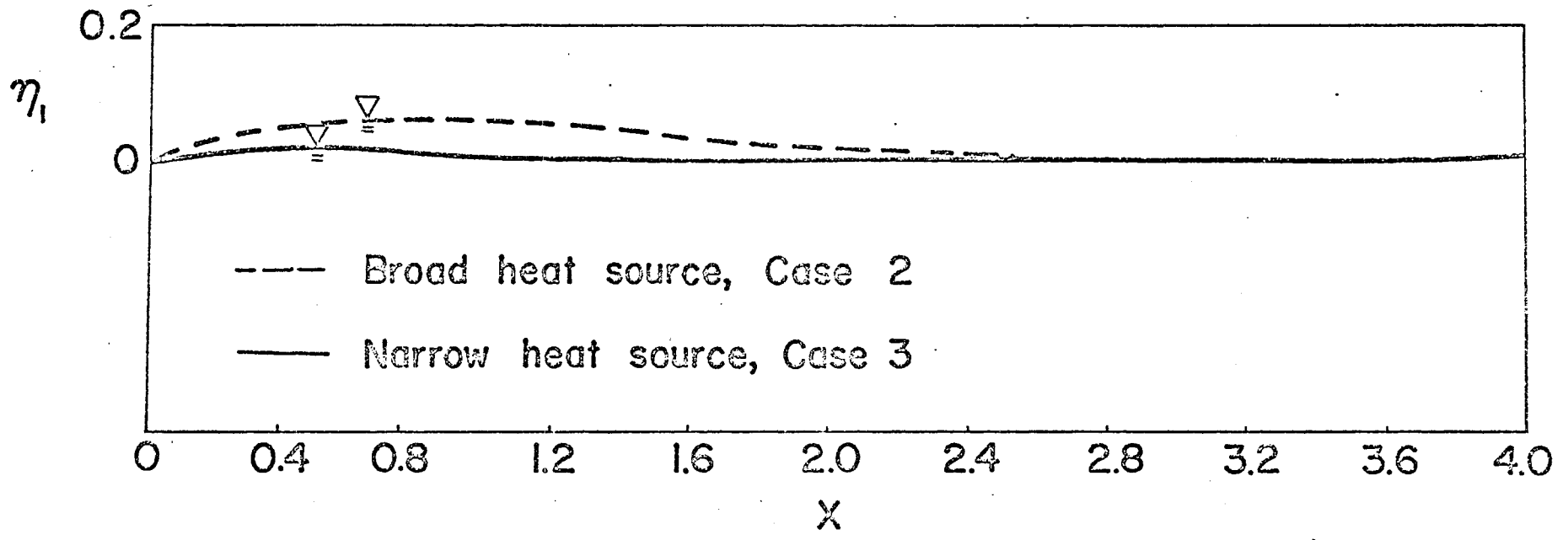


FIG. 7B. EFFECT OF THE SIZE OF THE HEAT SOURCE ON THE FIRST-ORDER PERTURBATION FUNCTION FOR THE UPWELLING OF WATER TABLE

APPENDIX A

ALTERNATIVE FORMULATION IN TERMS OF STREAM FUNCTION

In order to plot the streamline, we shall now reformulate the problem in terms of stream function. Eqs. (1) - (4) in terms of stream function are given by

$$\frac{\partial^2 \Psi}{\partial X^2} + \frac{\partial^2 \Psi}{\partial Y^2} = -\varepsilon \frac{\partial \Theta}{\partial X}, \quad (\text{A-1})$$

$$\frac{\partial^2 \Theta}{\partial X^2} + \frac{\partial^2 \Theta}{\partial Y^2} = D \left[\frac{\partial \Psi}{\partial Y} \frac{\partial \Theta}{\partial X} - \frac{\partial \Psi}{\partial X} \frac{\partial \Theta}{\partial Y} \right], \quad (\text{A-2})$$

where Ψ is the dimensionless stream function defined by $\Psi \equiv \frac{\mu \psi}{\rho_s g h K}$ and ψ is the dimensional stream function given by $u = \frac{\partial \psi}{\partial y}$ and $v = -\frac{\partial \psi}{\partial x}$.

The boundary condition for Ψ are given by

$$\frac{\partial \Psi}{\partial X} (0, Y) = 0, \quad (\text{A-3})$$

$$\frac{\partial \Psi}{\partial X} (L, Y) = 0, \quad (\text{A-4})$$

$$\Psi (x, \bar{\eta}) = 0, \quad (\text{A-5})$$

$$\Psi (x, 0) = 0, \quad (\text{A-6})$$

and the boundary conditions for Θ are given by Eq. (22).

We now apply the perturbation method by assuming that

$$\Psi (X, Y) = \sum_{m=0}^{\infty} \varepsilon^m \Psi_m (X, Y), \quad (\text{A-7})$$

$$\Theta (X, Y) = \sum_{m=0}^{\infty} \varepsilon^m \Theta_m (X, Y), \quad (\text{A-8})$$

$$\bar{\eta} (X) = 1 + \sum_{m=1}^{\infty} \varepsilon^m \eta_m (X). \quad (\text{A-9})$$

Substituting Eqs. (B-7) - (B-9) into Eqs. (B-1) - (B-4), expanding the boundary conditions in a Taylor's series and collecting like powers of ϵ , we have the following set of linear problems:

Zero-Order Approximations

$$\frac{\partial^2 \Psi_0}{\partial X^2} + \frac{\partial^2 \Psi_0}{\partial Y^2} = 0, \quad (A-10)$$

$$\frac{\partial \Psi_0}{\partial X} (0, Y) = 0, \quad (A-11)$$

$$\frac{\partial \Psi_0}{\partial X} (L_1, Y) = 0, \quad (A-12)$$

$$\Psi_0 (x, 1) = 0, \quad (A-13)$$

$$\Psi_0 (x, 0) = 0. \quad (A-14)$$

Thus the solution for Ψ_0 is $\Psi_0 = 0$, (A-15)

The zero-order approximation for temperature is

$$\frac{\partial^2 \theta_0}{\partial X^2} + \frac{\partial^2 \theta_0}{\partial Y^2} = D \left[\frac{\partial \Psi_0}{\partial Y} \frac{\partial \theta_0}{\partial X} - \frac{\partial \Psi_0}{\partial X} \frac{\partial \theta_0}{\partial Y} \right], \quad (A-16)$$

with boundary conditions given by Eq. (28).

First-Order Approximations

The first-order approximation for ψ is given by

$$\frac{\partial^2 \Psi_1}{\partial X^2} + \frac{\partial^2 \Psi_1}{\partial Y^2} = - \frac{\partial \theta_0}{\partial X_1}, \quad (A-17)$$

with boundary conditions given by

$$\frac{\partial \psi_1}{\partial X} (0, Y) = 0, \quad (\text{A-18})$$

$$\frac{\partial \psi_1}{\partial X} (L, Y) = 0, \quad (\text{A-19})$$

$$\psi_1 (x, 1) = 0, \quad (\text{A-20})$$

$$\psi_1 (x, 0) = 0. \quad (\text{A-21})$$

The first-order perturbation function for θ is given by

$$\frac{\partial^2 \theta_1}{\partial X^2} + \frac{\partial^2 \theta_1}{\partial Y^2} = \left[\frac{\partial \psi_1}{\partial Y} \frac{\partial \theta_0}{\partial X} - \frac{\partial \psi_1}{\partial X} \frac{\partial \theta_0}{\partial Y} \right], \quad (\text{A-22})$$

with boundary conditions given by

$$\theta_1 (0, Y) = 0, \quad (\text{A-23})$$

$$\theta_1 (L, Y) = 0, \quad (\text{A-24})$$

$$\theta_1 (X, 1) = - \frac{\partial \theta_0}{\partial Y} (X, 1) \eta_1 (X), \quad (\text{A-25})$$

$$\theta_1 (x, 0) = 0. \quad (\text{A-26})$$

APPENDIX B

FINITE DIFFERENCE EQUATIONS

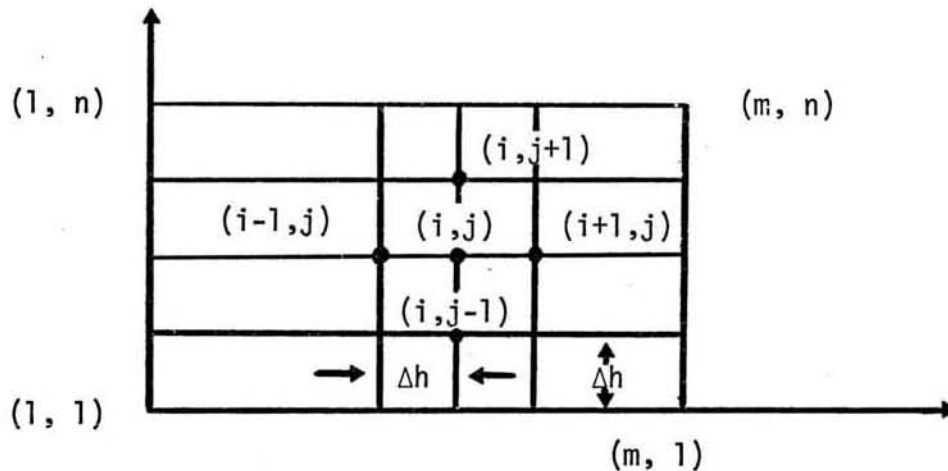
The Laplace Equation

$$\frac{\partial^2 \phi}{\partial X^2} + \frac{\partial^2 \phi}{\partial Y^2} = 0, \quad (B-1)$$

is replaced by the standard five-point formula

$$\phi_{i,j} = (1/4) \left[\phi_{i+1,j} + \phi_{i-1,j} + \phi_{i,j+1} + \phi_{i,j-1} \right], \quad (B-2)$$

where (i, j) denotes i th point along X-axis and j th point along Y-axis.



Similarly the Poisson Equation

$$\frac{\partial^2 \phi}{\partial X^2} + \frac{\partial^2 \phi}{\partial Y^2} = f(X, Y), \quad (B-3)$$

is replaced by the difference equation

$$\phi_{i,j} = (1/4) \left[\phi_{i+1,j} + \phi_{i-1,j} + \phi_{i,j+1} + \phi_{i,j-1} - \Delta h^2 f_{i,j} \right]. \quad (B-4)$$

Note that

$$X_i = (i - 1) \Delta h, \quad (B-5)$$

and

$$Y_j = (j - 1) \Delta h. \quad (B-6)$$

[1] The difference equations for θ_0 . The governing equation and boundary conditions for θ_0 are

$$\frac{\partial^2 \theta_0}{\partial X^2} + \frac{\partial^2 \theta_0}{\partial Y^2} = 0, \quad (B-7)$$

$$\theta_0 (X, 0) = \theta_L (X), \quad (B-8)$$

$$\theta_0 (X, 1) = \theta_a, \quad (B-9)$$

$$\theta_0 (0, Y) = 0, \quad (B-10)$$

$$\theta_0 (L, Y) = 0. \quad (B-11)$$

With the aid of Eq. (B-2), Eq. (B-7) is approximated by

$$(\theta_0)_{i,j} = (1/4) \left[(\theta_0)_{i+1,j} + (\theta_0)_{i-1,j} + (\theta_0)_{i,j+1} + (\theta_0)_{i,j-1} \right],$$

where $i = 2, \dots, m-1,$

$$j = 2, \dots, n-1. \quad (B-12)$$

From Eqs. (B-8) - (B-11), one obtains

$$(\theta_0)_{i,1} = (\theta_L)_i, \quad i = 1, \dots, m, \quad (B-13)$$

$$(\theta_0)_{i,n} = \theta_a, \quad i = 1, \dots, m, \quad (B-14)$$

$$(\theta_0)_{1,j} = 0, \quad j = 2, \dots, n-1, \quad (B-15)$$

$$(\theta_0)_{m,j} = 0, \quad j = 2, \dots, n-1. \quad (B-16)$$

[2] The difference equations for P_1 The governing equation and boundary conditions for P_1 are

$$\frac{\partial^2 P_1}{\partial X^2} + \frac{\partial^2 P_1}{\partial Y^2} = \frac{\partial \theta_0}{\partial Y}, \quad (\text{B-17})$$

$$\frac{\partial P_1}{\partial Y}(X, 1) = \theta_a, \quad (\text{B-18})$$

$$\frac{\partial P_1}{\partial Y}(X, 0) = \theta_L(X), \quad (\text{B-19})$$

$$P_1(0, Y) = 0, \quad (\text{B-20})$$

$$P_1(L, Y) = 0. \quad (\text{B-21})$$

Eq. (B-18) can be replaced by the following difference equation:

$$\frac{(P_1)_{i, n+1} - (P_1)_{i, n-1}}{2\Delta h} = \theta_a, \quad (\text{B-22})$$

or
$$(P_1)_{i, n+1} = (P_1)_{i, n-1} + 2\Delta h \theta_a. \quad (\text{B-23})$$

Eq. (B-19) can be replaced by the following difference equation:

$$\frac{(P_1)_{i, 2} - (P_1)_{i, 0}}{2\Delta h} = (\theta_L)_i, \quad (\text{B-24})$$

or
$$(P_1)_{i, 0} = (P_1)_{i, 2} - 2\Delta h (\theta_L)_i. \quad (\text{B-25})$$

Eq. (B-17) can be replaced by

$$(P_1)_{i,j} = (1/4) \left[(P_1)_{i+1,j} + (P_1)_{i-1,j} + (P_1)_{i,j+1} + (P_1)_{i,j-1} - \Delta h^2 (\theta_{0,\gamma})_{i,j} \right],$$

with $i = 2, \dots, m-1,$

$$j = 2, \dots, n-1, \quad (B-26)$$

where $(\theta_{0,\gamma})_{i,j}$ is $\frac{\partial \theta_0}{\partial \gamma}$ value at grid point (i, j) . From Eq. (B-20) one obtains

$$(P_1)_{1,j} = 0, \quad j = 1, \dots, n. \quad (B-27)$$

From Eq. (B-21) one obtains

$$(P_1)_{m,j} = 0, \quad j = 1, \dots, n. \quad (B-28)$$

Combining Eqs. (B-23) and (B-26) with $j = n$, one gets

$$(P_1)_{i,n} = (1/4) \left[(P_1)_{i+1,n} + (P_1)_{i-1,n} + 2(P_1)_{i,n-1} + 2\Delta h \theta_a - \Delta h^2 (\theta_{0,\gamma})_{i,n} \right],$$

$$\text{where } i = 2, \dots, m-1. \quad (B-29)$$

Combining Eqs. (B-25) and (B-26) with $j = 1$, one gets

$$(P_1)_{i,1} = (1/4) \left[(P_1)_{i+1,1} + (P_1)_{i-1,1} + 2(P_1)_{i,2} - 2\Delta h (\theta_L)_i - \Delta h^2 (\theta_{0,\gamma})_{i,1} \right],$$

$$\text{where } i = 2, \dots, m-1. \quad (B-30)$$

The set of difference equations for P_1 comprises Eqs. (B-26) - (B-30).

[3] The difference equations for θ_1

The governing equation and boundary conditions for θ_1 are

$$\frac{\partial^2 \theta_1}{\partial X^2} + \frac{\partial^2 \theta_1}{\partial Y^2} = -D \left[\frac{\partial P_1}{\partial X} \frac{\partial \theta_0}{\partial X} + \frac{\partial P_1}{\partial Y} \frac{\partial \theta_0}{\partial Y} - \theta_0 \frac{\partial \theta_0}{\partial Y} \right], \quad (\text{B-31})$$

$$\theta_1(X, 1) = -\frac{\partial \theta_0}{\partial Y}(X, 1) P_1(X, 1), \quad (\text{B-32})$$

$$\theta_1(X, 0) = 0, \quad (\text{B-33})$$

$$\theta_1(0, Y) = 0, \quad (\text{B-34})$$

$$\theta_1(L, Y) = 0. \quad (\text{B-35})$$

The advection term

$$f(X, Y) \equiv D \left[\frac{\partial P_1}{\partial X} \frac{\partial \theta_0}{\partial X} + \frac{\partial P_1}{\partial Y} \frac{\partial \theta_0}{\partial Y} - \theta_0 \frac{\partial \theta_0}{\partial Y} \right], \quad (\text{B-36})$$

is replaced by

$$f_{i,j} = D \left[(P_{1,X})_{i,j} (\theta_{0,X})_{i,j} + (P_{1,Y})_{i,j} (\theta_{0,Y})_{i,j} - (\theta_0)_{i,j} (\theta_{0,Y})_{i,j} \right]. \quad (\text{B-37})$$

Thus, the difference equation for Eq. (B-31) is

$$(\theta_1)_{i,j} = 1/4 \left[(\theta_1)_{i+1,j} + (\theta_1)_{i-1,j} + (\theta_1)_{i,j+1} + (\theta_1)_{i,j-1} + \Delta h^2 f_{i,j} \right]. \quad (\text{B-38})$$

From Eqs. (B-32) - (B-35) one obtains

$$(\theta_1)_{i, n} = - (\theta_0, \gamma)_{i, n} (P_1)_{i, n}, \text{ where } i = 1, \dots, m, \quad (\text{B-39})$$

$$(\theta_1)_{i, 1} = 0, \text{ where } i = 1, \dots, m, \quad (\text{B-40})$$

$$(\theta_1)_{1, j} = 0, \text{ where } j = 2, \dots, n - 1, \quad (\text{B-41})$$

$$(\theta_1)_{m, j} = 0, \text{ where } j = 2, \dots, w - 1. \quad (\text{B-42})$$

The set of difference equations for θ_1 comprises Eqs. (B-38) - (B-42).

[4] Finite difference equations for ψ .

The governing equation and boundary conditions for ψ are

$$\frac{\partial^2 \psi_1}{\partial X^2} + \frac{\partial^2 \psi_1}{\partial Y^2} = - \frac{\partial \theta_0}{\partial X}, \quad (\text{B-43})$$

$$\frac{\partial \psi_1}{\partial X} (0, \gamma) = 0, \quad (\text{B-44})$$

$$\frac{\partial \psi_1}{\partial X} (L, \gamma) = 0, \quad (\text{B-45})$$

$$\psi_1 (X, 1) = 0, \quad (\text{B-46})$$

$$\psi_1 (X, 0) = 0. \quad (\text{B-47})$$

Eq. (B-44) can be replaced by the following difference formula:

$$\frac{(\psi_1)_{2, j} - (\psi_1)_{0, j}}{2\Delta h} = 0, \text{ or } (\psi_1)_{2, j} = (\psi_1)_{0, j}. \quad (\text{B-48})$$

Eq. (B-45) gives

$$\frac{(\psi_1)_{m+1,j} - (\psi_1)_{m-1,j}}{2\Delta h} = 0, \text{ or } (\psi_1)_{m+1,j} = (\psi_1)_{m-1,j}. \quad (\text{B-49})$$

With Eq. (B-4), Eq. (B-43) can be expressed as

$$(\psi_1)_{i,j} = (1/4) \left[(\psi_1)_{i+1,j} + (\psi_1)_{i-1,j} + (\psi_1)_{i,j+1} + (\psi_1)_{i,j-1} + (\theta_{0,\chi})_{i,j} \Delta h^2 \right],$$

where $i = 2, \dots, m-1,$

$$j = 2, \dots, n-1. \quad (\text{B-50})$$

Eqs. (B-46) and (B-47) give

$$(\psi_1)_{i,n} = 0, \quad (\text{B-51a})$$

$$(\psi_1)_{i,1} = 0. \quad (\text{B-51b})$$

Combining Eqs. (B-48) and (B-50) with $i = 1,$ one gets

$$(\psi_1)_{1,j} = (1/4) \left[2(\psi_1)_{2,j} + (\psi_1)_{1,j+1} + (\psi_1)_{1,j-1} + \Delta h^2 (\theta_{0,\chi})_{1,j} \right], \quad (\text{B-52})$$

Combining Eqs. (B-49) and (B-50) with $l = m,$ one gets

$$(\psi_1)_{m,j} = (1/4) \left[2(\psi_1)_{m-1,j} + (\psi_1)_{m,j+1} + (\psi_1)_{m,j-1} + \Delta h^2 (\theta_{0,\chi})_{m,j} \right],$$

$$\text{where } j = 2, \dots, n-1. \quad (\text{B-53})$$

The set of difference equations for stream function ψ_1 then comprises Eqs. (B-50) - (B-53).

COMPUTER PROGRAMS

COMPILED BY W-2500 FORTRAN IV, REV. 6

PAGE 00

```

0001: C
0002: C I, THIS PROGRAM ITERATES THE TEMPERATURE ZERO-ORDER SOLUTION
0003: C
0004:     DIMENSION T(41,11), TL(41)
0005:     IIN=2
0006:     IDUT=3
0007:     M=41
0008:     N=11
0009:     XK=.1
0010:     XK=2.0
0011:     M1=M-1
0012:     N1=N-1
0013:     DH=1./FLOAT(N1)
0014:     TV=.02
0015:     ITER=0
0016:     DEKR=.001
0017:     X=0.0
0018:     DO 10 I=1,M
0019:     XKL=((X-XL)/XK)**2
0020:     IF(XKL.LE.20.) GO TO 11
0021:     TL(I)=0.04
0022:     GO TO 10
0023: 11   TL(I)=1./EXP(XKL) + .05
0024:     TL(I) = TL(I)/1.05
0025: 10   X=X+DH
0026:     WRITE(3,2)(TL(KL),KL=1,41)
0027: 2    FORMAT(2X,10F10.4)
0028:     DO 15 I=2,N1
0029:     DO 15 J=2,N1
0030:     TS=(TV-TL(I))/FLOAT(N1)
0031: 15   T(I,J)= TS*FLOAT(J)+TL(I)
0032:     DO 20 I=1,N
0033:     T(I,1)=0.
0034: 20   T(M,1)=0.
0035:     DO 30 I=2,M1
0036:     T(1,I)=TL(I)
0037: 30   T(1,N)=TV
0038:     WRITE(IDUT,150)
0039: 150  FORMAT('1','INITIAL VALUES')
0040:     WRITE(IDUT,151)((T(I,J),J=1,N),I=1,M)
0041: 151  FORMAT(2X,11F11.3)
0042: 50   DMAX=0.0
0043:     FMAX=0.0
0044:     ITER=ITER+1
0045:     DO 50 I=2,M1
0046:     DO 50 J=2,N1
0047:     TEMP=T(I,J)
0048:     T(I,J)=(T(I+1,J)+T(I-1,J)+T(I,J+1)+T(I,J-1))/4.
0049:     DIFF=ABS(T(I,J)-TEMP)
0050:     DABV=ABS(T(I,J))
0051:     IF(DABV.GT.FMAX)FMAX=DABV
0052:     IF(DIFF.GT.DMAX)DMAX=DIFF
0053: 50   CONTINUE
0054:     DDIF=DMAX/FMAX

```

```
0055:      IF(DDIF.GT.DERR) GO TO 60
0056:      WRITE(IOUT,152) ITER,FMAX,DMAX,DDIF
0057: 152  FORMAT('1','CONVERGENCE ON ITERATION ',I3,2X,'FUNCTIONAL MAXIMUM
0058: C ',F10.3/2X,'ABS MAXIMUM DIFFERENCE ',F6.3,2X,'PERCENTAGE DIFFI
0059: CRENCE ',F6.4)
0060:      WRITE(IOCT,153)XR,XL
0061: 153  FORMAT('0', 'TEMPERATURE O WITH XK=',F4.2,' AND XL=',F4.2//)
0062:      WRITE(IOCT,151)((T(I,J),J=1,N),I=1,M)
0063:      CALL CREATE(100,'TEMPPFILE')
0064:      DO 1010 I=1,M
0065: 1010  WRITE(100)(T(I,J),J=1,N)
0066:      REWIND 102
0067:      STOP
0068:      END
```

```

0001: C
0002: C   E. THIS PROGRAM CALCULATES THE PARTIAL DERIVATIVES OF THETA 0
0003: C
0004:     DIMENSION T(41,11),TY(41,11),TI(41),TO(41)
0005:     M=41
0006:     N=11
0007:     CALL CREATE(102,'TPDYFILE')
0008:     CALL OPEN(100,'TEMPFILE')
0009:     READ(100)((T(I,J),J=1,N),I=1,M)
0010:     WRITE(5,2)
0011: 2     FORMAT('1',' THE TEMPERATURE FUNCTION ')
0012:     IO=3
0013:     IN=2
0014:     WRITE(10,1)((T(I,J),J=1,N),I=1,M)
0015: 1     FORMAT(' ',3X,11F11.3)
0016:     DH=1.0/FLOAT(N-1)
0017:     DO 100 I=1,M
0018:     DO 105 J=1,N
0019:     TI(J)=T(I,J)
0020: 105    CONTINUE
0021:     CALL DET5(DH,TI,TO,N,IER)
0022:     DO 100 J=1,N
0023:     TY(1,J)=TO(J)
0024: 100    CONTINUE
0025:     DO 120 I=1,M
0026:     WRITE(102)(TY(1,J),J=1,N)
0027: 120    CONTINUE
0028: 3     FORMAT('1',' THE DERIVATIVE OF TEMPERATURE WITH RESPECT TO Y ')
0029:     WRITE(5,3)
0030:     WRITE(10,1)((TY(1,J),J=1,N),I=1,M)
0031:     DO 200 J=1,N
0032:     DO 205 I=1,M
0033:     TI(I)=T(I,J)
0034: 205    CONTINUE
0035:     CALL DET5(DH,TI,TO,M,IER)
0036:     DO 200 I=1,M
0037:     TY(I,J)=TO(I)
0038: 200    CONTINUE
0039: 7     FORMAT('1',' THE DERIVATIVES OF TEMPERATURE 0 WITH RESP TO X')
0040:     CALL CREATE(100,'TPDXFILE')
0041:     DO 210 I=1,M
0042:     WRITE(100)(TY(1,J),J=1,N)
0043: 210    CONTINUE
0044:     WRITE(10,7)
0045:     WRITE(10,1)((TY(1,J),J=1,N),I=1,M)
0046:     STOP
0047:     END

```

```
0001: C      SUBROUTINE DETS
0002:      SUBROUTINE DET5(H,Y,Z,NDIM,IER)
0003:      DIMENSION Y(41),Z(41)
0004:      IF(NDIM-5)4,1,1
0005: 1      IF(H)2,5,2
0006: 2      HH=.08333333/H
0007:      YY=Y(NDIM-4)
0008:      B=HH*(-25.*Y(1)+48.*Y(2)-36.*Y(3)+16.*Y(4)-3.*Y(5))
0009:      C=HH*(-3.*Y(1)-10.*Y(2)+18.*Y(3)-6.*Y(4)+Y(5))
0010:      DO 3 I=5,NDIM
0011:      A=B
0012:      B=C
0013:      C=HH*(Y(I-4)-Y(I)+8.*(Y(I-1)-Y(I-3)))
0014: 3      Z(I-4)=A
0015:      IER=0
0016:      A=HH*(-YY+6.*Y(NDIM-3)-18.*Y(NDIM-2)+10.*Y(NDIM-1)+3.*Y(NDIM))
0017:      C2(NDIM)=HH*(3.*YY-16.*Y(NDIM-3)+36.*Y(NDIM-2)-48.*Y(NDIM-1)
0018: 1      +25.*Y(NDIM))
0019:      Z(NDIM-1)=A
0020:      Z(NDIM-2)=C
0021:      Z(NDIM-3)=B
0022:      RETURN
0023: 4      IER=-1
0024:      RETURN
0025: 5      IER=-1
0026:      RETURN
0027:      END
```

```

0001: C
0002: C   THIS PROGRAM ITERATES THE PRESSURE FIRST-ORDER SOLUTION
0003: C   PROGRAM FOR PRESSURE1
0004: C
0005:       DIMENSION P(41,11),T(41),TY(41,11)
0006:       DATA P/451*0.0/
0007:       IN=2
0008:       IU=3
0009:       XK=0.1
0010:       XK=2.0
0011:       M=41
0012:       N=11
0013:       M1=M-1
0014:       N1=N-1
0015:       DH=1.0/FLD0AT(N1)
0016:       ITER=0
0017:       DERR=0.001
0018:       X=0.
0019:       DO 10 I=1,N
0020:         XKL=((X-XL)/XK)**2
0021:         IF(XKL.LE.20.) GO TO 11
0022:         T(I)=0.04
0023:         GO TO 10
0024: 11     T(I)= 1./EXP(XKL) + .05
0025:         T(I)= T(I)/1.05
0026: 10     X=X+DH
0027:         CALL OPEN(100,'TPDYFILE')
0028:         DO 12 I=1,N
0029:           READ(100) (TY(I,J),J=1,N)
0030: 12     CONTINUE
0031: 15     DMAX=0.0
0032:         FMAX=0.0
0033:         DO 20 I=2,M1
0034:           DO 20 J=1,N1
0035:             TEMP=P(I,J)
0036:             IF(J.EQ.1)GO TO 25
0037:             IF(J.EQ.N)GO TO 26
0038:             P(I,J)=P(I+1,J)+P(I-1,J)+P(I,J-1)+P(I,J+1)-DH*DH*TY(I,J)
0039:             P(I,J)=0.25*P(I,J)
0040:             GO TO 30
0041: 25     P(I,1)=P(I+1,1)+P(I-1,1)+2.*P(I,2)-2.*DH*T(I)-DH*DH*TY(I,1)
0042:             P(I,1)=P(I,1)*0.25
0043:             GO TO 30
0044: 26     P(I,N)=P(I+1,N)+P(I-1,N)+2.*P(I,N1)+2.*DH*0.02-DH*DH*TY(I,N)
0045:             P(I,N)=0.25*P(I,N)
0046: 30     DABV=ABS(P(I,J)-TEMP)
0047:             DFAB=ABS(P(I,J))
0048:             IF(DABV.GT.DMAX)DMAX=DABV
0049:             IF(DFAB.GT.FMAX)FMAX=DFAB
0050: 20     CONTINUE
0051:         DABV=DMAX/FMAX
0052:         ITER=ITER+1
0053:         IF(DABV.GT.DERR)GO TO 15
0054:         WRITE(10,5)

```



```
0055: 5   FORMAT('1',' THE PRESURE FUNCTION - P1'///)
0056:      DO 50 I=1,M
0057: 50   WRITE(10,6)(P(I,J),J=1,N)
0058: 6   FORMAT(' ',3X,11F11.3)
0059:      WRITE(10,7)ITER
0060: 7   FORMAT(/// 4X,'ITERATION CONVERGES AFTER',I4,'TRIES')
0061:      CALL CREATE(102,'PRSIFILE')
0062:      DO 100 I=1,M
0063:      WRITE(102)(P(I,J),J=1,N)
0064: 100   CONTINUE
0065:      STOP
0066:      END
```

```

0001: C
0002: C IV THIS PROGRAM CALCULATES THE PARTIAL DERIVATIVES OF PRESSURE 1
0003: C
0004: DIMENSION T(41,11),TY(41,11),TI(41),TO(41)
0005: M=41
0006: N=11
0007: CALL CREATE(102,'PIDYFILE')
0008: CALL OPEN(100,'PRSIFILE')
0009: READ(100)((T(I,J),J=1,N),I=1,M)
0010: WRITE(3,2)
0011: 2 FORMAT('1',' THE PRESSURE - P1 FUNCTION')
0012: IO=3
0013: IN=2
0014: WRITE(IO,1)((T(I,J),J=1,N),I=1,M)
0015: 1 FORMAT('1',3x,11F11.3)
0016: DH=1.0/FLOAT(N-1)
0017: DO 100 I=1,M
0018: DO 105 J=1,N
0019: TI(J)=T(I,J)
0020: 105 CONTINUE
0021: CALL DET5(DH,TI,TO,N,IER)
0022: DO 100 J=1,N
0023: TY(I,J)=TO(J)
0024: 100 CONTINUE
0025: DO 120 I=1,M
0026: WRITE(102)(TY(I,J),J=1,N)
0027: 120 CONTINUE
0028: 3 FORMAT('1',' THE VALUE OF D(P1) / DY')
0029: WRITE(3,3)
0030: WRITE(IO,1)((TY(I,J),J=1,N),I=1,M)
0031: DO 200 J=1,N
0032: DO 205 I=1,M
0033: TI(I)=T(I,J)
0034: 205 CONTINUE
0035: CALL DET5(DH,TI,TO,M,IER)
0036: DO 200 I=1,M
0037: TY(I,J)=TO(I)
0038: 200 CONTINUE
0039: 7 FORMAT('1',' THE VALUE OF D(P1) / DX')
0040: CALL CREATE(100,'PIDXFILE')
0041: DO 210 I=1,M
0042: WRITE(100)(TY(I,J),J=1,N)
0043: 210 CONTINUE
0044: WRITE(IO,7)
0045: WRITE(IO,1)((TY(I,J),J=1,N),I=1,M)
0046: STOP
0047: END

```

```

0001: C
0002: C THIS PROGRAM CALCULATES THE ADVECTION TERM IN THE THETA 1 EQUATION
0003: C
0004: DIMENSION CUN(41,11),FA(41,11),FB(41,11)
0005: DATA N/41/,N/11/,IN/2/,IE/3/
0006: 1 FORMAT(' ',3X,11F11.3)
0007: 2 FORMAT('1',' THE D(TO) / DX FUNCTION')
0008: 3 FORMAT('1',' THE D(P1) / DX FUNCTION')
0009: 4 FORMAT('1',' THE D(P1) / DY FUNCTION')
0010: 5 FORMAT('1',' THE D(TO) / DY FUNCTION')
0011: 6 FORMAT('1',' THE TO FUNCTION')
0012: ITER=0
0013: DISCH=1000.
0014: NI=M-1
0015: N1=N-1
0016: DH=1./FLOAT(N1)
0017: CALL OPEN(100,'PIDXFILE')
0018: READ(100)((FA(I,J),J=1,N),I=1,M)
0019: WRITE(10,3)
0020: WRITE(10,1)((FA(I,J),J=1,N),I=1,M)
0021: CALL OPEN(100,'TPOXFILE')
0022: READ(100)((FB(I,J),J=1,N),I=1,M)
0023: WRITE(10,2)
0024: WRITE(10,1)((FB(I,J),J=1,N),I=1,M)
0025: DO 500 I=1,M
0026: DO 500 J=1,N
0027: CUN(I,J)=FA(I,J)*FB(I,J)
0028: 500 CONTINUE
0029: CALL OPEN(100,'PIDYFILE')
0030: READ(100)((FA(I,J),J=1,N),I=1,M)
0031: WRITE(10,4)
0032: WRITE(10,1)((FA(I,J),J=1,N),I=1,M)
0033: CALL OPEN(100,'TPOYFILE')
0034: READ(100)((FB(I,J),J=1,N),I=1,M)
0035: WRITE(10,5)
0036: WRITE(10,1)((FB(I,J),J=1,N),I=1,M)
0037: DO 600 I=1,M
0038: DO 600 J=1,N
0039: CUN(I,J)=CUN(I,J)+FA(I,J)*FB(I,J)
0040: 600 CONTINUE
0041: CALL OPEN(100,'TEMPFILE')
0042: READ(100)((FA(I,J),J=1,N),I=1,M)
0043: WRITE(10,6)
0044: WRITE(10,1)((FA(I,J),J=1,N),I=1,M)
0045: DO 850 I=1,M
0046: DO 850 J=1,N
0047: CUN(I,J)=CUN(I,J)-FA(I,J)*FB(I,J)
0048: CUN(I,J)=CUN(I,J)*DISCH*DH*DH
0049: 850 CONTINUE
0050: WRITE(10,13)
0051: 13 FORMAT('1',' THE CONSTANT FUNCTION')
0052: WRITE(3,502) DISCH
0053: 502 FORMAT('0', 'DISCHARGE = ',F6.0)
0054: CALL CREATE(100,'CONSTANT')

```

```
0055:      WRITE(10,1)((CLN(I,J),J=1,N),I=1,M)
0056:      DO 610 I=1,M
0057:      WRITE(100)(CLN(I,J),J=1,N)
0058: 610   CONTINUE
0059:      STOP
0060:      END
```

```

0001: C
0002: C THIS PROGRAM ITERATES THE TEMPERATURE FIRST-ORDER SOLUTION
0003: C
0004: C PROGRAM FOR THERM1
0005: DIMENSION FA(41,11),FB(41,11),CON(41,11)
0006: DATA Fb/451*0.0/
0007: 1 FORMAT(4X,11F11.3)
0008: 2 FORMAT('1',' THE INPUT CONSTANT FUNCTION')
0009: 3 FORMAT('1',' THE TEMPERATURE')
0010: IG=3
0011: N=41
0012: M=11
0013: M1=M-1
0014: N1=N-1
0015: CALL OPEN(103,'TPDYFILE')
0016: CALL OPEN(104,'PKSIFILE')
0017: DO 20 I=1,N
0018: READ(103) (FA(I,J),J=1,N)
0019: READ(104) (CON(I,J),J=1,N)
0020: 20 FB(I,N)=-(FA(I,N)*CON(I,N))
0021: CALL OPEN(100,'CONSTANT')
0022: READ(100)((CON(I,J),J=1,N),I=1,M)
0023: WRITE(IG,2)
0024: WRITE(IG,1)((CON(I,J),J=1,N),I=1,M)
0025: CALL OPEN(100,'TEMPFILE')
0026: READ(100)((FA(I,J),J=1,N),I=1,M)
0027: WRITE(IG,3)
0028: WRITE(IG,1)((FA(I,J),J=1,N),I=1,M)
0029: 900 DMAX=0.
0030: FMAX=0.
0031: DO 700 I=2,M1
0032: DO 700 J=2,N1
0033: TEMP=FB(I,J)
0034: FB(I,J)=FB(I+1,J)+FB(I-1,J)+FB(I,J+1)+FB(I,J-1)+CON(I,J)
0035: FB(I,J)=0.25*FB(I,J)
0036: DAB=ABS(FB(I,J)-TEMP)
0037: FAB=ABS(FB(I,J))
0038: IF(DAB.GT.DMAX)DMAX=DAB
0039: IF(FAB.GT.FMAX)FMAX=FAB
0040: 700 CONTINUE
0041: ITER=ITER+1
0042: DAB=DMAX/FMAX
0043: IF(DAB.GT.0.001)GO TO 900
0044: 11 FORMAT('1',' THE T1 FUNCTION')
0045: 12 FORMAT('C',' AFTER',I5,' ITERATIONS')
0046: WRITE(IG,11)
0047: WRITE(IG,12)ITER
0048: WRITE(IG,1)((FB(I,J),J=1,N),I=1,M)
0049: CALL CREATE(100,'TEMPERFL')
0050: DO 2000 I=1,N
0051: 2000 WRITE(100)(FB(I,J),J=1,N)
0052: CALL CREATE(100,'TEMPERFL')
0053: DO 800 I=1,M
0054: DO 800 J=1,N

```

```
0055:      CON(I,J)=FA(I,J)+FB(I,J)*0.1
0056: 800   CONTINUE
0057:      DO 910 I=1,M
0058:      WRITE(100)(CON(I,J),J=1,N)
0059: 910   CONTINUE
0060:      WRITE(10,6)
0061: 6      FORMAT('1',' THE T0 + T1 FUNCTION')
0062:      WRITE(10,1)((CON(I,J),J=1,N),I=1,M)
0063:      STOP
0064:      END
```

```
0001: C
0002: C  II. THE PROGRAM TO COMPUTE  $P_0 + E \cdot P_1$ 
0003: C
0004:      DIMENSION P1(41,11),P(41,11)
0005: 1     FORMAT(' ',3X,11F11.5)
0006: 2     FORMAT('1',' THE PRESURE FUNCTION')
0007:      CALL OPEN(100,'PKS1FILE')
0008:      N=41
0009:      N=11
0010:      DH=1.0/FLOAT(N-1)
0011:      DO 10 I=1,41
0012:      READ(100)(P1(I,J),J=1,11)
0013: 10     CONTINUE
0014:      Y=0.
0015:      DO 15 J=1,11
0016:      DO 20 I=1,41
0017:      P(I,J)=1.0-Y
0018: 20     CONTINUE
0019:      Y=Y+DH
0020: 15     CONTINUE
0021:      DO 30 I=1,N
0022:      DO 30 J=1,N
0023:      P(I,J)=P(I,J)+P1(I,J)*0.1
0024: 30     CONTINUE
0025:      CALL CREATE(102,'PRESSURE')
0026:      WRITE(3,2)
0027:      DO 50 I=1,N
0028:      WRITE(102)(P(I,J),J=1,N)
0029:      WRITE(3,1)(P(I,J),J=1,N)
0030: 50     CONTINUE
0031:      STOP
0032:      END
```

```

0001: C
0002: C THIS PROGRAM ITERATES THE STREAM FUNCTION I
0003: C
0004: C PROGRAM FOR STREAM FUNCTION
0005: DIMENSION P(41,11), TX(41,11)
0006: DATA P/451*0.0/
0007: IN=2
0008: IO=3
0009: M=41
0010: N=11
0011: M1=M-1
0012: N1=N-1
0013: DH=1.0/FLOAT(N1)
0014: ITER=0
0015: DERR=0.001
0016: CALL OPEN(100,'TPDXFILE')
0017: DO 12 I=1,M
0018: READ(100) (TX(I,J),J=1,N)
0019: 12 CONTINUE
0020: 15 DMAX=0.0
0021: FMAX=C.C
0022: DO 20 I=1,M
0023: DO 20 J=2,N1
0024: TEMP=P(I,J)
0025: IF(I.EQ.1) GO TO 25
0026: IF(I.EQ.M) GO TO 26
0027: P(I,J)=P(I+1,J) + P(I-1,J) + P(I,J-1) + P(I,J+1) + DH*DH*TX(I,J)
0028: P(I,J)=0.25*P(I,J)
0029: GO TO 30
0030: 25 P(I,J)=P(I,J-1) + P(I,J+1) + 2.*P(2,J) + DH*DH*TX(I,J)
0031: P(I,J)=P(I,J)*0.25
0032: GO TO 30
0033: 26 P(M,J) = P(M,J-1) + P(M,J+1) + 2.*P(M1,J) + DH*DH*TX(M,J)
0034: P(M,J) = P(M,J)*0.25
0035: 30 DABV=ABS(P(I,J)-TEMP)
0036: DFAB=ABS(P(I,J))
0037: IF(DABV.GT.DMAX) DMAX=DABV
0038: IF(DFAB.GT.FMAX) FMAX=DFAB
0039: 20 CONTINUE
0040: DABV=DMAX/FMAX
0041: ITER=ITER+1
0042: IF(DABV.GT.DERR) GO TO 15
0043: WRITE(IO,5)
0044: 5 FORMAT('1', ' THE STREAM FUNCTION'///)
0045: DO 50 I=1,M
0046: 50 WRITE(IO,6) (P(I,J),J=1,N)
0047: 6 FORMAT(' ',3X,11F11.3)
0048: WRITE(IO,7) ITER
0049: 7 FORMAT(//// 4X,' ITERATION CONVERGES AFTER',14,' TRIES')
0050: CALL CREATE(102,'STREAMF1')
0051: DO 100 I=1,M
0052: WRITE(102) (P(I,J),J=1,N)
0053: 100 CONTINUE
0054: STOP

```